Materials Today Sustainability 27 (2024) 100812

Contents lists available at ScienceDirect

Materials Today Sustainability

journal homepage: www.journals.elsevier.com/materials-today-sustainability

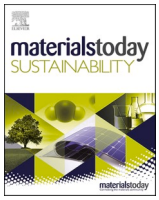

A comprehensive review of metal-organic frameworks sorbents and their mixed-matrix membranes composites for biogas cleaning and CO_2/CH_4 separation

Zama Duma [a,*], Peter R. Makgwane [a,b,**], Mike Masukume [a], Ashton Swartbooi [a], Khavharendwe Rambau [a], Thembelihle Mehlo [a], Tshidzani Mavhungu [a]

[a] HySA Infrastructure Centre of Competence, Centre for Nanostructure and Advanced Materials (CeNAM), Council for Scientific and Industrial Research (CSIR), Pretoria, 0001, South Africa
[b] Institute for Catalysis and Energy Solutions (ICES), College of Science Engineering and Technology (CSET), University of South Africa, Private Bag X6, Florida, 1710, South Africa

ARTICLE INFO

Keywords:
Metal-organic frameworks
Sorbents
Membranes
Mixed-matrix membranes
Biogas
Adsorption
Carbon capture

ABSTRACT

Metal-organic framework (MOF) sorbent materials have recently gained considerable attention in gas separation technology. This is because of their unique structural properties, such as high gas permeability and selectivity promoted by large porosity and high surface areas. Integrating MOF fillers with polymer membranes to construct mixed-matrix membranes (MMMs) has enhanced gas separation and capture performance and stability. This review provides a comprehensive current status development in MOFs and their integrated MMMs composites with focused applications in biogas cleaning for the removal of common trace impurities such as hydrogen sulfide (H_2S), ammonia (NH_3), siloxanes, and moisture and upgrading of the subsequent carbon dioxide/methane (CO_2/CH_4) mixture to bio-methane and biogenic CO_2. We highlight the structural properties and descriptors critical for designing MOF sorbents and MOF-based MMMs to improve their adsorption capacities and separation efficiency in biogas cleaning and upgrading. The tuneable surface modifications of MOFs boasted by the surface-endowed basic-acidic sites and coordinated open metal sites effectively provide high adsorption capacities and separation selectivities in biogas processing. The combination of MOFs and membranes offers high separation efficiencies of biogas-derived CO_2 and CH_4 for their diverse potential downstream utilisation. Future perspectives on advancing further developments in MOF sorbents and MOFs-based MMMs for biogas cleaning and upgrading to access sustainable and green derivatives with fewer carbon footprints while beneficiating wastes for adopting a circular economy are highlighted to provide solutions to the shortcomings.

1. Introduction

The world is moving towards decarbonisation, with various countries making pledges to reduce carbon emissions to mitigate climate impact and ensure future sustainable energy and a clean environment [1–7]. Renewable energy sectors such as wind and solar have also expanded worldwide, giving a glimpse of a net-zero climate [8–10]. Biogas falls under the renewable energy umbrella as a biofuel and is used to complement the well-known renewable energy systems [11,12]. Biogas can be produced through anaerobic digestion, where microorganisms degrade organic materials without oxygen. Biogas constituents mainly depend on the digested organic matter and digestion conditions. The standard components of biogas are primarily methane (CH_4, 40–75%), carbon dioxide (CO_2, 15–60%), hydrogen sulfide (H_2S, 0.005–2%), siloxanes (0–0.02%), ammonia (NH_3,0–100 ppm), oxygen (O_2, 0–1%), carbon monoxide (CO, <0.6%) and nitrogen (N_2, 0–2%) [13]. The elevated content of CH_4 makes biogas an attractive energy source, and countries such as Germany and China have adopted biogas to produce electricity, heat, and steam for households and industries and included it in the natural gas grid [14,15].

* Corresponding author. Institute for Catalysis and Energy Solutions (ICES), College of Science Engineering and Technology (CSET), University of South Africa, Private Bag X6, Florida, 1710, South Africa
** Corresponding author. HySA Infrastructure Centre of Competence, Centre for Nanostructure and Advanced Materials (CeNAM), Council for Scientific and Industrial Research (CSIR), Pretoria, 0001, South Africa.
E-mail addresses: zduma@csir.co.za (Z. Duma), makgwpr@unisa.ac.za, makgwane.peter@gmail.com (P.R. Makgwane).

https://doi.org/10.1016/j.mtsust.2024.100812
Received 20 January 2024; Received in revised form 15 April 2024; Accepted 6 May 2024
Available online 7 May 2024

Unfortunately, the drawback of raw biogas preventing its direct use in energy generation and chemical feedstock is its constituents other than CH_4, which requires prior cleaning to elevate its properties. For example, CO_2 and N_2 decrease the CH_4 specific calorific value and Wobbe index [16,17]. O_2 increases the explosion hazard, while NH_3 and H_2O can cause corrosion within the turbines during combustion [18–20]. H_2S is amongst the more hazardous constituents of raw biogas; it is corrosive, flammable, and toxic to humans and animals. A low concentration, such as 5 ppm, can cause respiratory and neurological symptoms, making it a health hazard [21–23]. Furthermore, for biogas-derived CO_2 conversions into green chemicals such as methanol, dimethyl ether, and organic acids via catalyst-driven hydrogenation or reduction, a trace of H_2S needs to be removed because of its adverse effects on the performance of the catalysts. Specifically, H_2S and sulfur derivatives (e.g., SO_2) in biogas can affect the performance of the sorbent materials for biogas CO_2/CH_4 upgrading or cause poising to catalyst active sites in the typical CO_2 and CH_4 valorisation reaction, hence desulfurisation of biogas before upgrading and valorisation.

H_2S can be removed from biogas through pre-digestion, during digestion, and post-digestion. For pre-and during digestion, the H_2S concentration can only be removed up to a certain level and thus still needs cleaning post-digestion, hence the increase in emphasis on digestion cleaning/removal [24,25]. Post-digestion cleaning includes membrane separation, cryogenic distillation, absorption, and adsorption [26–29]. Membrane separation technology works on selective permeability towards H_2S using specific membranes while retaining CH_4. Cryogenic distillation involves liquifying gases at high pressures and low temperatures based on boiling points [26–29]. The absorption process consists of the absorption of H_2S in a liquid, either physically or chemically. Physical absorption involves dissolving the H_2S in a solvent, and chemical absorption involves dissolving H_2S and a subsequent chemical reaction between H_2S and a low solvent [30]. Adsorption consists of capturing the gases on a high surface area solid. Adsorption technology is one of the most influential and competitive methods for H_2S removal. An effective adsorbent material must have high surface area and porosity, good sorption capacity and kinetics, and be regenerable [31,32].

Metal-organic frameworks (MOFs) have emerged as an attractive class of nanoporous materials possessing well-structured cavities with confinement effects suitable for various applications in gas separation [33–36], gas capture, catalysis [37–40], energy generation [41–44] and energy storage [45–47]. Due to their profound structure-enhanced performances in diverse applications, MOFs have recently emerged as attractive materials in biogas clean-up and upgrading [48]. Interestingly, in the application of MOFs for biogas impurities clean-up and upgrading or separation of CO_2/CH_4, MOFs can be used as sorbents and membranes integrated with enhanced performance efficiencies because of their high surface areas, porosity, flexible surface functionalities, and cavity structure architecture. Previous studies have reviewed the application of MOFs and MOFs-based mixed-matrix membranes (MMMs) in biogas clean-up [49,50]. Review articles focusing only on the capture or adsorption and storage of biogas-derived CO_2 and air CO_2 have been reported [51–55]. Recently, Khan et al. has reported a comprehensive MOFs-based MMMs review for biogas CO_2/CH4 [56]. The reported work focused mainly on application milestones' engineering and commercial aspects. In this review, we provide a comprehensive current status development in MOFs-based sorbent materials and their integrated MMMs technologies with focused utilisation in biogas impurities cleaning removal and upgrading of CO_2/CH_4 gas mixture. The scope of this review starts with providing an overview of the biogas value chain while highlighting the need to purify and upgrade it before utilising its derivative product streams of CO_2 and CH_4 as feedstock for energy and chemicals. It further discusses brief structural properties and classification of commonly known MOFs, including the general synthesis methodologies that have been established. Furthermore, the application performance of neat and modified MOFs in removing biogas impurities, including upgrading CO_2/CH_4, is critically presented. Finally, the adaptation of MOF filler integration in the membrane technology to develop advanced MMM systems is highlighted by comparing performance to those of neat MOFs and membranes. Finally, the review provided the updated status of MOFs and their counterpart's integrated MMM systems for biogas cleaning and upgradation separation of CO_2/CH_4 and highlighted perspectives on future research directions to pursue better MOFs-based materials for practical potential applications.

2. Biogas refinery concept

Fig. 1 depicts a tentative process flow diagram of a biorefinery conceptual value chain that can be built around biogas utilisation with some of the features relating to clean-up and upgrading. Generally, organic municipal waste is fed to anaerobic digesters where biological processes break down the organic matter to generate a raw biogas stream, mainly comprised of CH_4 and CO_2 as major constituents. The biogas can also present trace contaminants such as H_2S, NH_3, siloxanes, moisture, and air. A liquid digestate rich in nutrients can also be produced with a biogas stream, which can be used as a crop fertiliser. In a typical biogas process environment, the steps include chilling (i.e., to remove moisture), biological desulphurisation (to remove H_2S), and lastly, passing over a sorbent material (e.g., activated carbon bed) to remove unwanted siloxanes [57–60]. These processes can also be accomplished through adsorption and chemisorption onto highly porous materials, some activated, resulting in lower operating expenses (OPEX) costs than water scrubbing [61,62]. The cleaned biogas is then taken to an upgrading unit, where the CO_2 component is removed to maximise the calorific value of the biogas. The result is a pure stream of bio-methane, which has the same characteristics as natural gas, and a concentrated stream of CO_2 [61]. This stream of CO_2 can then undergo activation through the reverse water-gas shift reaction to produce syngas, an essential feedstock for Fischer-Tropsch synthesis in the petroleum and chemical industry [63,64]. Similarly, CO_2 can be directly converted to alcohols, olefins, and hydrocarbons for chemicals and fuel energy [65].

Bio-methane can be injected into suitable natural gas pipelines or used directly as a replacement fuel in compressed natural gas-driven vehicles [66,67]. Bio-methane can also be used as a feedstock in the pyrolysis and reforming methane for syngas and hydrogen production [68–70]. In such reaction processes, both hydrogen gas and solid carbons are formed over a catalyst [71–73]Hydrogen can be further used for energy applications, in fuel cells, or as a feedstock to produce green chemicals. Depending on the type of catalyst used, the solid carbons formed during the pyrolysis reaction can either be low-grade amorphous carbons or high-valued carbon nanostructures. These, in turn, can be used as high-surface-area adsorbents.

Lastly, since bio-methane is a direct replacement for natural gas, it can also be used as a substitute feedstock in the petrochemical industry that relies on natural gas reforming to produce syngas. In such operations, it presents an excellent opportunity to achieve decarbonisation to some extent. Consequently, biogas should be considered an essential feedstock to decarbonise several industries since it can provide feedstock to multiple sectors. While the scale of biogas production would not reach the quantities needed for large operations, partial feedstock substitution would allow industry sectors to decarbonise faster. Using biogas, two greenhouse gases (i.e., CO_2/CH_4) are captured and utilised in processes, resulting in greener products with minimal environmental release. This speaks to a fully circular economy built around utilising organic municipal waste that usually goes to landfills.

3. Brief classification of MOF materials

MOFs are characterised by metal centres inter-connected by various organic linkers to create one-, two-, and three-dimensional porous

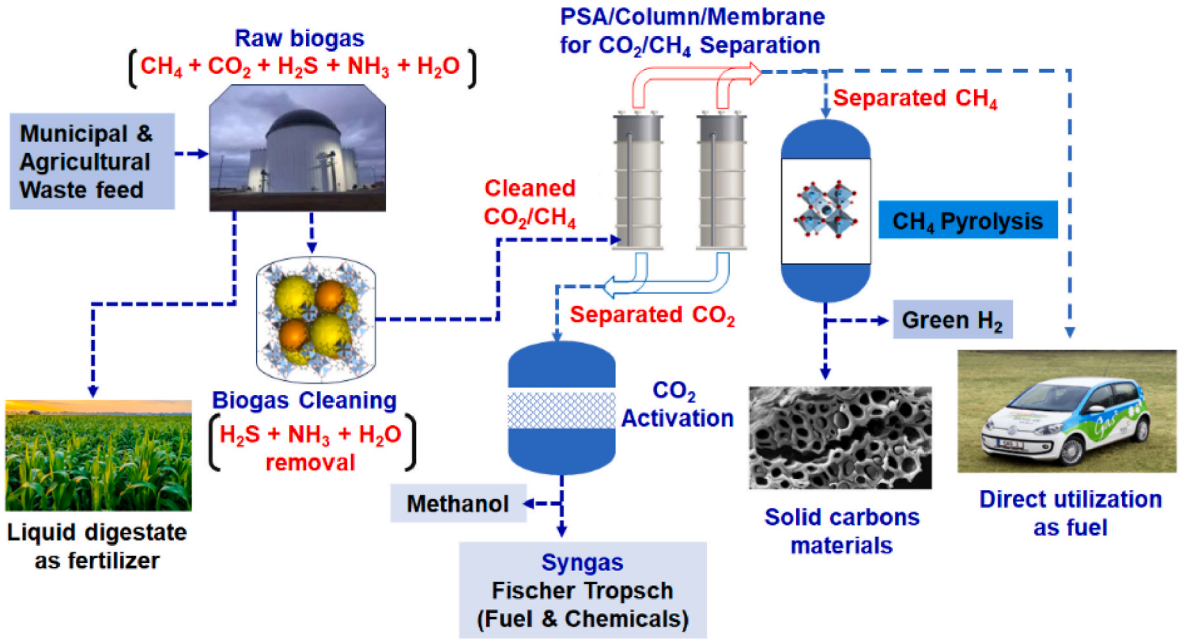

Fig. 1. Value-chain diagram of biogas generation, clean-up, upgrade, and valorisation.

structure architectures with tuneable pore volumes and pore diameters ranging between 3 and 20 Å, leading to ultra-high surface areas and surface chemical properties. Many MOF materials have been designed and synthesised, and their numbers continue to increase with the introduction of new ones. Table 1 summarises some common MOFs well-established in the literature and have been practically evaluated in diverse applications, including biogas cleaning and upgrading.

The synthesis of MOFs generally employs a combination of metal ions and organic linkers in the presence of a solvent, as illustrated schematically in Fig. 2. The most common conventional methods to synthesise MOFs are based on hydrothermal and solvothermal routes [74–80]. Unconventional methods such as the mechanochemical method involving solventless mixing of metal ions and organic linker by grinding using a mortar and pestle or ball milling have also been reported successfully with the benefits of rapid short reaction times in a range of 10–60 min [81–84]. Alternatively, both microwave-assisted synthesis and sonochemical processes with ultrasonic radiation (20 kHz–10 MHz) have been implemented successfully in the synthesis of MOFs with beneficial advantages such as rapid crystallisation times, phase selectivity, control of small particle size distribution and morphology [85–90]. While we only presented a panoramic overview of the MOF materials basics with respect to structure properties and their synthesis descriptors, for detailed information on the various synthesis methods and strategies of MOF materials, readers are encouraged to read comprehensive focused reviews such as UiO [91,92]], MIL [93], ZIF [94,95], HUASK [96] and others. Furthermore, other comprehensive synthesis methods reviewed with a special focus on MOF-based hierarchically porous materials [97,98], and green synthesis of MOF [99], mechanochemistry for green synthesis of MOFs [84], bimetallic nanoparticles/MOFs [100] are available.

Table 1
Summary of most common MOF materials available in the literature.

MOF class	Building blocks constituents	Examples
Materials Institute Lavoisier (MIL)	MIL MOFs are based on trivalent metal ions (Fe^{3+}, Al^{3+}, Ga^{3+}, Cr^{3+}, Va^{3+}, In^{3+}) and carboxylic acid ligands.	MIL-53, MIL-100, and MIL-88, MIL-101, and MIL-125.
University of Oslo (UiO)	UiO MOFs are based on dicarboxylic acid building units, $Zr_6(\mu_3\text{-}O)_4(\mu_3\text{-}OH)$ metal precursors, and an organic linker.	UiO-66, UiO-67, UiO-68, and UiO-69
Zeolitic Imidazolate Frameworks (ZIFs)	ZIFs are based on metal ions with valence electrons (Zn, Fe, Cu, Co) and imidazole derivatives as linkers.	ZIF-8, ZIF-90, ZIF-L, ZIF-71, ZIF-67, ZIF-7.
Isoreticular MOFs (IRMOFs)	Isoreticular MOFs are synthesised by $[Zn_4O]^{6+}$ as building units and various aromatic carboxylates.	MOF-5 or IRMOF-1
Hong Kong University of Science and Technology (HKUST)	Are derived from the metal precursor of copper and benzene tricarboxylic acid (trimesic acid)	HKUST-1 or MOF-199 (Cu-BTC)

4. MOFs sorbents for biogas impurities cleaning

Removing trace impurities in biogas and upgrading or separating the clean mixture of biogas CO_2/CH_4 stream can be achieved via physisorption and chemisorption. The surface functionalities of the sorbent materials are critical to establishing the mode of contact between the biogas constituents and the adsorption materials to determine whether such interaction proceeds with physisorption or chemisorption. As illustrated in Fig. 3, several parameters control the physisorption and chemisorption processes. Furthermore, physisorption occurs when an intermolecular force exists between the adsorbate and the adsorbent. When the intermolecular force of interaction is weak, physisorption can be reversible to a certain extent [101]. On the other hand, chemisorption occurs when there is an electron transfer between the adsorbate and adsorbent material to form a chemical bond interaction [102]. Strong acidic-basic site interactions usually promote chemisorption, coordination bonds between metal and gas molecules, and ionic and covalent bonds. It is an irreversible process, thus leading to permanent alteration in their electronic structures.

4.1. Removal of moisture

The removal of moisture is one of the critical stages in biogas clean-up. Removing water content or air in the biogas should be the first step to avoid its impact on the sorbent materials for the subsequent removal of H_2S [104,105]. There have been reports that showed the presence of

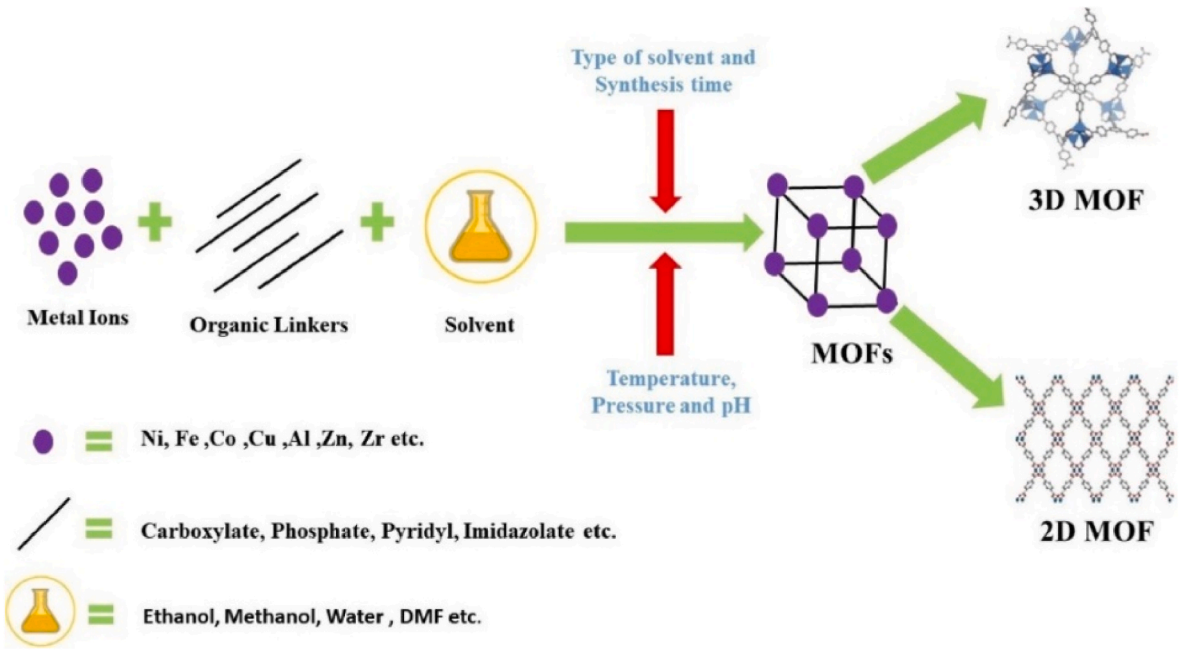

Fig. 2. General illustration of MOF synthesis. Ref. [56].

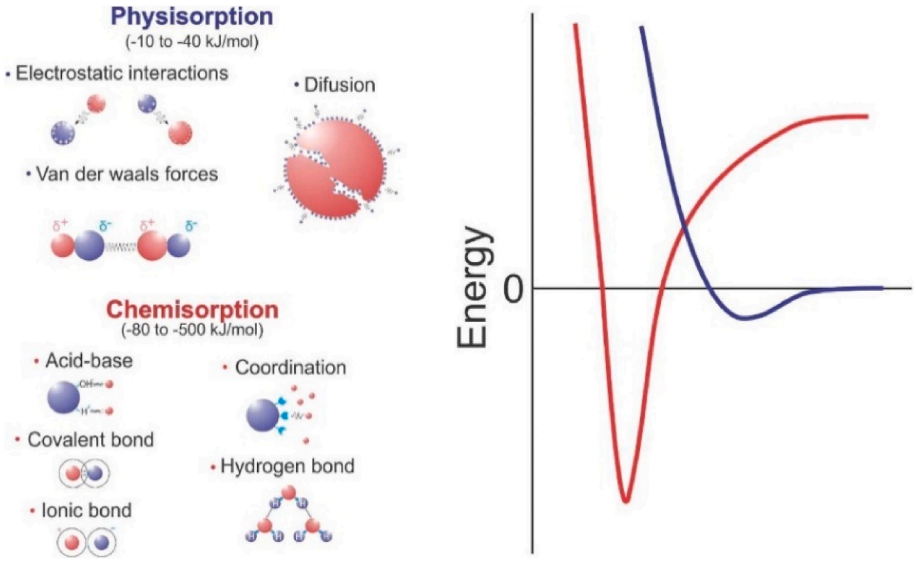

Fig. 3. Schematic physisorption and chemisorption processes and their respective operational properties. Reprinted from Ref. [103].

moisture in biogas to have a significant effect on the efficiency of removal of H_2S [106]. Furthermore, the reaction of H_2O and CO_2 has the potential to generate trace amounts of carbonic acid that could eventually be corrosive. Generally, a biogas cleaning setup features a moisture trap column before an H_2S removal column. Sometimes, a single material can perform multipurpose tasks such as removing moisture, siloxanes, and H_2S, and it can also be used in a fixed-bed column for CO_2/CH_4 upgrading. The application of MOFs in moisture removal from biogas is limited in the literature. However, MOFs have demonstrated a significant breakthrough application in harvesting atmospheric moisture for the potential generation of clean water for human consumption [107–112]. As a result, it can be expected that the adoption of such preliminary success in capturing/absorbing atmospheric water could be applicable in removing moisture during biogas cleaning and upgrading. The MOF application targeted toward moisture removal in biogas is still developing.

4.2. *Removal of NH_3 gas*

Organic matter that has been anaerobic digested usually contains NH_3 as an impurity [113]. To improve the quality and suitability of biogas for various applications, the removal of NH_3 is pivotal. Adsorption is a well-established method for NH_3 removal using everyday materials such as zeolites, activated carbon, and porous organic polymers [114–116]. MOFs have recently been demonstrated as promising sorbent materials for NH_3, and they have often shown better performance than their predecessors, owing to their structural diversity, large porosity, and high surface areas [117–120].

A variety of functionalized zirconia based UiO-66 MOFs such as UiO-66-OH, UiO-66-$(OH)_2$, UiO-66-NO_2, UiO-66-NH_2, UiO-66-SO_3H, and UiO-66-$(COOH)_2$ were evaluated for their performance towards NH_3 removal during air purification [121]. According to the results, UiO-66-SO_3H and UiO-66-$(COOH)_2$ were less effective in NH_3

adsorption activity than UiO-66-OH and UiO-66-NH_2. In the presence of bulky functional groups, such as –COOH and –SO_3H, the framework porosity (i.e., surface area and pore volume) significantly decreased. The –OH group interacted strongly with NH_3 and was the least bulky among the functional groups. The adsorption capacity of UiO-66-OH for NH_3 under dry conditions was found to be 5.7 mmol/g. Under humid conditions, functionalized UiO-66 MOFs showed a decrease in NH_3 adsorption capacity. A study by Glomb et al. [122] demonstrated that urea-functionalized dicarboxylic acid enhances the NH_3 uptake of UiO-66 MOF by 17.8 mmol/g. Other researchers also conducted a study using synthesised Manchester Framework Material (MFM)-300(Al) for NH_3 adsorption, which resulted in an adsorption capacity of 15.7 mmol/g and reversible adsorption after 50 cycles [120]. These long-term performance studies were reported under dry conditions, albeit it is still being determined whether humid conditions will yield significant performance improvements.

Using a volumetric measurement at 298 K and NH_3 pressures up to 1 bar, Saha et al. [104] measured the equilibrium and kinetics of Zn-based MOF-5 and MOF-177 MOFs. It was found that MOF-177 absorbs more NH_3 than MOF-5 when NH_3 pressures are below 0.2 bar, and at 1 bar, both MOFs adsorb NH_3 about the same magnitude (~12.2 mmol/g). Based on the adsorption results, it was demonstrated that physical adsorption of NH_3 on MOFs dominates when NH_3 pressures are below 0.2 bar, after which a chemical reaction between NH_3 and the MOF frameworks occurs, reducing surface area and pore volume. In another study, NH_3 sorption was reported by Moribe et al. for three reticular porphyrin-based MOFs, namely, Al-PMOF, Ga-PMOF, and In-PMOF, where metal rod primary building units were coupled with Brønsted acidic bridging hydroxyl groups [123]. The reversibility of adsorption activity was observed on the sorption isotherms of NH_3 in Al-PMOF. Furthermore, Ga-PMOF and In-PMOF showed steeper adsorption isotherm slopes than Al-PMOF at lower-pressure regions, with decreased NH_3 adsorbed between the first and second cycles [123]. MIL-160, CAU-10-H (Aluminum isophthalate [Al(OH)(bdc)]·nH 2 O), Al-Fum (aluminium fumarate), and MIL-53(Al) MOFs were studied to capture and store NH_3 [124]. The results from this study performed at 298 K and 1.0 bar exhibited NH_3 uptakes of 12.8 mmol/g for MIL-160 followed by 10.0 mmol/g for CAU-10-H, then 8.9 mmol/g for Al-Fum and lastly, 3.0 mmol/g for MIL-53(Al).

In the other study, the structural degradation of highly stable MOFs after the adsorption of NH_3 was evaluated, and it was shown that the integral molecular structure collapsed post-exposure to the NH_3 gas [119,125]. The reversible storage and adsorption of NH_3 by MFM-300 (Al) MOF have also been investigated [120]. When MFM-300(Al) MOF was operated at 273 K and 1.0 bar, it showed an NH_3 uptake of 15.7 mmol/g and a packing density of 0.70 g cm^{-3} when compared with the liquid density of NH_3 (0.681 g cm^{-3}) at 240 K. In addition, the packing density of NH_3 at 293 K is also impressive at 0.62 g cm^{-3}. Additionally, MFM-300(Al) exhibited complete reversibility under conventional pressure swing adsorption (PSA) conditions, with no loss in storage capacity after 50 cycles of adsorption and desorption. While MOFs are challenging, they remain viable as sorbents for potential applications in removing NH_3 from biogas. Apart from MOF properties of large pores, high surface areas, and open metal sites, their tuneable surfaces of Brønsted and Lewis acid/bases sites provide unique structure properties for enhanced adsorption of NH_3. The developments of MOFs specific to biogas NH_3 removal still require further research aiming at designing MOF properties that could allow adsorptive removal of all trace impurities using single MOFs before CO_2/CH_4 upgrading or perhaps perform all such desirable biogas impurities removal and upgrade in a single MOF composite material.

4.3. Removal of siloxanes

Siloxanes are chemical compounds of Si–O groups with oxygen atoms attached to organic radicals such as methyl, phenyl, vinyl, and ethyl [126]. They are applied in cosmetic product formulations for softening, deodorants, rubber, oils, and food additives [9]. The presence of siloxanes in biogas originates from landfill sites and municipal waste derivatives. Furthermore, their presence in biogas can have a detrimental effect during combustion [127,128]. For example, the gaseous siloxanes inside the combustion turbine or transport engine precipitate to form oxides. These residues are highly abrasive and can cause wearing and rusting of the engine's metal components if the biogas is used as fuel without pre-cleaning [127]. Table 2 lists some representatives of the different types of siloxanes in biogas.

There are few studies focused on the adsorptive removal of siloxanes from biogas. Mito-oka et al. conducted a survey of siloxane D4 adsorption using both DUT-4 (Dresden University of Technology 4) and Zn_4O(bdc)(bpz)^2] MOFs with hydrophobic nature and high surface areas by exposing them to siloxane D4 for over 3.5 h at 30 °C [129]. Based on the TGA results, the adsorption capacity of DUT-4 was measured to be 15 wt % and 30 wt% for Zn_4O(bdc)(bpz)^2]. The post-adsorption analysis of the MOFs showed high structural integrity, which confirmed their good stability and ability for regeneration. By using Si NMR, authors confirmed the chemical shift of the Si atoms in both DUT-4 and Zn_4O(bdc)(bpz)^2], which showed that they possessed high affinity toward siloxane D4 adsorption as corroborated by their high release temperatures of up to 250 °C. This behaviour was attributed to the interaction relationship between siloxanes and the MOFs, in which the pores of the frameworks play a critical role. For example, [Zn_4O(bdc)(bpz)^2] has neck-type shaped 3D connected channels, whereas DUT-4 has rhombic-shaped 1D straight channels, which are identical to the shapes of the adsorbed molecules. Under kinetic conditions with 50% relative humidity at 25 °C, the MOF's adsorption performance was better when compared to conventional materials such as activated carbon to achieve the siloxane removal efficiency of over 70% after 1000 min [129].

Table 3 summarises some of the most promising hydrophobic MOF materials in siloxane adsorption. Gargiulo et al. studied the adsorption of siloxane D4 on MIL-101 (Cr) and its regeneration behaviour in thermal treatment [130]. MIL-101 (Cr) had a saturation capacity of 3.2 mol/kg, which is higher than other reported materials. The high surface area and large micropores significantly enhanced the high adsorption capacities. MIL-101 (Cr) retained its structural integrity and was fully regenerated with heating at 423K under vacuum after prolonged exposure to siloxane D4 adsorption. The accessible active sites of MIL-101 (Cr) due to evacuated water molecules connected to the trimeric chromium (III) octahedral clusters accounted for high adsorption activity. These active sites inhibited the coordination of siloxane D4 molecule with hydrogen to avoid polymerisation, which showed a physisorption phenomenon. Due to these active sites, the adsorption isotherm from the Langmuir equation showed a strong affinity between MIL-101 (Cr) and siloxane D4. The MIL-101 (Cr) has already been demonstrated to be a promising adsorbent for H_2S, and the results from siloxane D4 adsorption open opportunities for its potential application in the simultaneous removal of H_2S and siloxane.

Gulcay-Ozcan et al. investigated several MOFs to find the best-performing MOF that does not require thermal treatment under vacuum for regeneration by correlating computational and experimental results [131]. Firstly, the authors conducted the Computation-Ready Experimental (CoRE) screening analysis of the MOF data for

Table 2
Some of the volatile methylsiloxanes are present in biogas [126].

Name	Abbreviation	Molecular structure
Hexamethyl-disiloxane	L2	$C_6H_{18}OSi_2$
Octamethyl-trisiloxane	L3	$C_8H_{24}O_2Si_3$
Decamethyl-tertasiloxane	L4	$C_{10}H_{30}O_3Si_4$
Hexamethylcyclo-trisiloxane	D3	$C_6H_{18}O_3Si_3$
Octamethylcyclo-tetrasiloxane	D4	$C_8H_{24}O_4Si_4$
Decamethylcyclo-pentasiloxane	D5	$C_{10}H_{30}O_5Si_5$
Dodecamethylcyclo-hexasiloxane	D6	$C_{12}H_{36}O_6Si_6$

Table 3
Top 10 promising hydrophobic MOFs identified for D4 uptake at 298 K [131].

MOF	Surface area (m^2/g)	Pore volume ($cm^3\ g^{-1}$)	Gravimetric uptake D4 (gg^{-1})	Volumetric uptake D4 (gcm^{-3})
FOTNIN (PCN-777)	2990	3.31	2.68	0.72
RUTNOK	6200	3.72	2.57	0.62
CUSYAR	5700	3.65	2.35	0.59
WUHDAG	5500	2.99	2.01	0.58
HOHMEX	5000	2.74	1.97	0.63
ECOKAJ	3600	2.68	1.97	0.65
DAJWET	5000	3.06	1.93	0.54
RUBDUP	4200	2.90	1.93	0.58
WUHCUZ	5500	2.91	1.80	0.54
ADATAC	5130	2.57	1.68	0.57

hydrophobic materials with a high D4 adsorption capacity as compared to the one reported by Gargiulo et al. (i.e., MIL-101 (Cr)). The identified hydrophobic MOFs were then narrowed to 10 selected MOF types due to their predicted high gravimetric siloxane D4 uptake. The standard features within the chosen MOFs were the void fraction (φ) greater than 0.81, pore volume higher than 1.7 cm^3/g, and highest D4 uptakes ranging from 1.68 to 2.68 g/g (Table 3). The best performing MOF amongst the 10 selected was FOTNIN (also known as PCN-777), which exhibited a predicted siloxane D4 gravimetric uptake of 2.68 g/g and volumetric uptake of 0.72 g cm^{-3} due to its high pore volume and large mesoporous cages (33.7 Å × 28.4 Å) [131]. The adsorption isotherm of FOTNIN was characterised by a V-shaped profile with a maximum uptake of 1.8 g/g (0.49 g/cm), which was higher than reported for DUT-4 and MIL-101(Cr). However, it was lower than the theoretical computational uptake due to a lower pore volume from inadequate pore evacuation and small windows of super-tetrahedral cages that inhibited siloxane D4 complete adsorption [131]. The FOTNIN showed 5 wt% less adsorption capacity after the first regeneration cycle due to D4 molecules trapped on the few defect sites. However, the second cycle showed repeatability with the same condensation pressure, total uptake, and no further capacity loss, thus indicating the stability of the material. To gain an in-depth understanding of the adsorption mechanism of the MOFs, authors used continuous fractional component Monte Carlo (CFCMC) simulations with OH/H_2O moieties of the Zr6 node on the MOF initially acting as primary adsorption sites. On the other hand, the siloxane D4 molecule has a heat of adsorption ranging from 65 to 75 kJ/mol, which is lower than the DUT-4 (194.0 kJ/mol), thus indicating that the adsorption energetics for PCNC-777 played a role in complete adsorption and reversibility. As the siloxane D4 adsorption loading increases, the molecules assemble in a monolayer close to the cage walls of the MOFs due to their interaction with the organic and inorganic linker nodes. The final stage is a higher D4 loading, where multilayers are formed, including occupation cages associated with capillary condensation [131].

4.4. Removal of H_2S gas

4.4.1. Pristine MOFs for H_2S removal

Physical treatment, such as adsorption, is highly effective in cleaning any sulfur-containing compound because H_2S can be chemically or physically adsorbed. Generally, the best adsorbent must possess good physicochemical properties such as high surface area, large pores and size distribution, and well-defined micropores to enable high-volume adsorbate uptake [132–134]. One of the early reports for the removal of H_2S from biogas using MOFs was reported by Hamon et al. [135]. The H_2S adsorption performance was tested on various MIL-based MOF types of MIL-47(V), MIL-100(Cr), MIL-101(Cr), and MIL-53 (Cr, Al, Fe). The ML-101 and MIL-100 MOFs with rigid and large pores achieved respectively maximum adsorption capacities of 16.7 and 38.4 mmol/g at operating pressures of 20 bar, while MIL-47 (V) had a maximum adsorption capacity of 14.6 mmol/g. Furthermore, the MIL-53(Cr, Al, Fe) MOFs showed a two-step adsorption isotherm, with respective maximum adsorption capacities of 13.12, 11.77, and 8.53 mmol/g. These uptake values for MIL-53 (Cr, Al. Fe) were attained at the second step of adsorption promoted by the smaller pore sizes. It has been established that when completely degassed, the MIL-53 family has an open pore structure, which closes at the low gas dosage and opens for high-pressure dosage, thus providing a "breathing effect". H_2S, as a polar molecule, interacts with the OH groups of the inorganic chain of the MIL-53 sorbent material, which subsequently leads to pore closure. In pore opening, the H_2S adsorption loading pressure should be high, which assists in facilitating the disintegration of the formed H_2S–OH bond and overall pore filling having weak interaction. According to the structural analysis results after adsorption studies, the structure intact of MIL-53(Fe) was destroyed due to the formation of iron sulfide and crystallisation of the organic linker. This confirmed that the chemosorption mechanism rather than physisorption was operational. Both MIL-47(V) and MIL-53(Al, Cr) MOFs exhibited physisorption phenomena through a complete regeneration in vacuum at 393K for 8 h compared to MIL-53(Fe). On the other hand, the MIL-100 and MIL-101 MOFs exhibited partial irreversibility, which is proposed to be either from partial structure framework deterioration or strong H_2S and OH group bond adsorption interactions. Another study evaluated the removal performance of H_2S from biogas by using 11 different MOFs based on MOF-5, MOF-74 (Mg, Zn), ZIF-8, UIO-66, M-BTC (Cu, Fe, Ce), and CU-BDC(ted) by comparing their respective adsorption breakthrough experiments with density functional theory (DFT) analyses [136]. Amongst the evaluated MOFs, few exhibited the physisorption phenomenon, which indicated the character of reversibility in their adsorption activity. For example, Mg-MOF-74 showed good stability when exposed to H_2S with an uptake of 0.24 mmol/g. After the regeneration process, the crystal structure of Mg-MOF-74 was still stable to maintain a high H_2S uptake. The stability of Mg-MOF-74 was attributed to the effect of a strong Mg–O carboxylate bond and a large gap between the Mg and S atoms, which was further confirmed by computational molecular dynamic simulation analysis that demonstrated the S(H_2S)–Mg distance of 2.8 Å to corroborate the physical adsorption mechanism [136]. Another example of well-established MOF, UiO-66, demonstrated a moderate removal H_2S uptake of 0.234 mmol/g with good reversible uptake adsorption activity. The UiO-66 has strong Zr–O bonds, and computational simulation studies showed that the adsorption of H_2S occurs in the middle of the tetrahedron cage of aromatic fragments structure, which is distant from the Zr-metal ion. These aromatic fragments of the UiO-66 structure have a potential field effect due to the sp^2 carbon that leads to its interaction with H_2S [136]. ZIF-8 MOF showed a reversible activity albeit poor H_2S uptake of 0.05 mmol/g compared to other MOFs because of its Zn atoms, which are completely bonded to the N atoms, thus leaving no other active site. Based on computational simulations studies, it was shown that there is a splitting energy of the d-orbital due to Zn atoms adopting the tetrahedral coordinated structure [136]. This implies that the electrons from H_2S cannot overlap to break the Zn–N bond, thus allowing the maintenance of the structure integrity of ZIF-8. A MOF based on highly redox cerium (Ce), Ce-BTC had a higher reversible H_2S uptake activity adsorption of 0.126 mmol/g, better than ZIF-8. The retaining of the Ce-BTC structural integrity was due to the division of f and d orbitals into considerable parts with low energy overlapping to sp orbital of O carboxylates, which is attributed to strong Ce–O carboxylates bond defending against H_2S corrosion [136]. On the other hand, MOFs such as Zn-MOF-74, MOF-5, and Cu-BTC, amongst others, demonstrated irreversible H_2S adsorption activities due to the disintegration of their respective structures. For example, Zn-MOF-74, with an H_2S uptake of 1.64 mol/g in the first cycle, displayed a decreased uptake of up to 0.043 mmol/g after regeneration. This was due to the deformed open sites of Zn-MOF-74 that allowed the H_2S interaction due to the compromised weak bond on O

hydroxyl-Zn-*O*-Carboxylate [136]. MOF-5 had a relatively high uptake of 1.11 mmol/g, which decreased to 0.04 mmol/g after regeneration. Like ZIF-8, the Zn atoms of the MOF-5 adopted a tetrahedral coordinated structural deformation. However, the d orbital of Zn and sp orbital of O MOF-5 was proposed to be less overlapping, thus leading to weaker bond energy of Zn–O. The Cu-BTC MOF or HKUST-1, with H_2S uptake of 1.1 mmol/g, displayed a change in colour from deep blue to dark during adsorption because the Cu metal preference to react with the S atom of the H_2S to form CuS which is difficult to desorb at moderate temperatures. The Cu atom and S have a matched d and p orbital that can form a strong covalent bond with a lower energy level, making it easy for the Cu–O carboxylate bonds to break in the structure framework of Cu-BTC MOF [136].

The disadvantage of irreversible activity of H_2S-exposed sorbents is a severe concern that prompted many recent studies to focus on searching for easily regeneratable materials such as MOF sorbents to remove H_2S from biogas efficiently. For example, Gupta et al. studied the stability and regeneration of different Cu-based MOFs synthesised via ultrasound, such as Cu-BDC, Cu-BTC, and Cu-BDC-N [137]. Cu-BDC demonstrated the highest H_2S uptake adsorption capacity of 105.6 mg/g, followed by Cu-BTC, then Cu-BDC with an uptake of 1.3 mg/g. When the pristine MOF material was exposed to moisture, its uptake seemed to increase significantly due to the dissolution of H_2S. The regeneration process was conducted by treating the exposed MOF material with methanol and UV radiation. Cu-BTC showed the highest uptake after regeneration of 95.6 mg/g, and Cu-BDC with an uptake of 31.3 mg/g. UV radiation enables the MOFs to go through a photolytic-decarboxylation process, which enhances their initial nature, aiding the adsorption of acidic gases such as H_2S.

4.4.2. *Modified MOFs for H_2S removal*

Modifying MOFs is one of the strategies used to improve the adsorption capacities of the parent pristine MOF materials, and most modified MOFs consist of a solid dispersive force that allows minor molecule retention [138]. Bhoria et al. functionalized HKUST-1 and HKUST-1/graphite oxide (GO) composite with polyethyleneimine (PEI) that is characterised by high amine density and free primary amine site at the end of its structure chain [139]. The PEI functionalized HKUST-1 had low H_2S adsorption performance because the PEI polymeric chains inhibited its pores. In contrast, HKUST-1/GO with functionalized PEI had higher adsorption of H_2S with an 80% increment compared to the neat HKUST-1. The high adsorption performance of the PEU/HKUST-1/GO composite was attributed to the improved uniform dispersion of MOF crystals on the functionalized GO surface and the PEI functionalities having a solid bond to GO, which ensured that the pores of HKUST-1 were not blocked. Furthermore, the amine group of PEI consists of long chains capable of increasing the interstitial spaces between GO layers, thus creating a composite of HKUST-1 to give entry to more active sites. The effect of GO in the GO/HKUST-1 composite to improve porosity for adsorption was also demonstrated by Petit et al. in a study involving the H_2S adsorption removal performance of hybrid HKUST-1 and GO composites prepared in situ with the GO with various loading amounts ranging from 5 to 46 wt% [140]. The pristine HKUST-1 had an H_2S adsorption capacity of 92 mg/g. At the same time, all the prepared hybrid composites demonstrated improved uptake, with the highest being 199 mg/g achieved with HKUST-1/GO composite containing 5 wt% of GO. The introduction of GO segmentally modified the HKUST-1 framework, which led to an increased porosity and surface area for improved H_2S adsorption capacity. Using activated carbon (AC), Shi et al. fabricated MOF-199/AC modified composites with AC loadings ranging from 1% to 3.5 % [141]. The MOF-199/AC composite with two wt% AC achieved the highest H_2S adsorption capacity of 8.46 % with a longer breakthrough time than other composites and the pristine MOF-199. Besides high surface area and increased porosity, AC possesses surface oxygen groups that can form chemical links between the MOF metallic centre and the AC functional groups. Kooti et al. investigated the effect of high-loading amounts of nanoporous carbons (NPc) of 10, 30, and 50% on the performance of modified MIL-101 (Cr)/NPc composite [142]. The MIL-101/NPC composite consisting of 30% loading of NPc achieved the highest H_2S uptake of 7.9 mmol/g, less than the neat MIL-101 (Cr) with an uptake of 10 mmol/g. It was observed that the difference in the packing density of the MIL-101/NPc composite compared to pristine MIL-101 played a significant role in the achieved adsorption capacities. Liu et al. studied the amino-functionalized UiO-66 compared to neat UiO-66 and other MOF materials [136]. The UiO-66-NH_2 MOF achieved a higher uptake than the pristine UiO-66 with an uptake of 0.909 mmol/g and maintained its structural integrity. However, after regeneration, the adsorption capacity of UiO-66-NH_2 was decreased to 0.38 mmol/g, which was due to the NH_2 group not being activated, thus could easily be reactive with H_2S to form NH_4HS that is difficult to decompose even upon heating without destroying the materials structure integrity. Apart from modifying MOFs with carbon-based materials, metal oxides have also demonstrated significant improvements in enhancing the H_2S adsorption capacities of MOF composites compared to pristine MOFs. Daraee et al. studied TiO_2/UiO-66 composites with various TiO_2 loadings to achieve the highest uptake of 0.21 g S/g [143]. The introduction of TiO_2 in UiO-66 increased the presence of the active site of Ti on UiO-66, leading to high adsorption capacity. In the study by Zou et al. [64], the interactions activity of various MOFs including MOF-74 (Mg, Zn), MOF-5, ZIF-8, MIL-101(Cr), UiO-66, UiO-66-NH_2, Cu-BDC(ted)$_{0.5}$ and M-BTC (M = Cu, Fe, and Ce) characterised by various structure properties of open metal sites, ligands, porosity and surface areas with H_2S were evaluated (Fig. 4).

5. MOFs sorbents for separation of biogas CO_2/CH_4

To increase the specific calorific value of biomethane, separation from CO_2 is warranted [144]. There is a myriad of proven technologies for CO_2 removal from biogas, including (i) water scrubbing, (ii) cryogenic distillation, (ii) chemical and physical absorption, (iv) membrane separation, and (v) pressure swing adsorption (PSA). The PSA system makes use of sorbent materials (e.g., zeolites, activated carbons, etc.) that serve as molecular sieves to separate gaseous molecules based on size difference to achieve high-purity streams of CH_4 (96–98%) [145]. Amongst the PSA-based sorbent materials, MOFs, because of their high

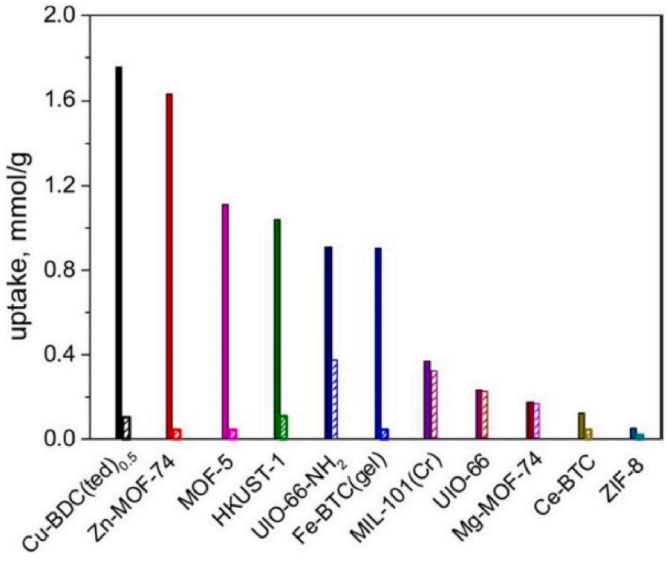

Fig. 4. Comparison of the performance of various MOF materials for H_2S uptake at 298 K (1 atm) and H_2S partial pressure of 1000 Pa. Filled column = H_2S uptake of fresh MOFs. Striped column = H_2S uptake of regenerated MOFs. Reprinted from Ref. [103].

surface area and porosity, have recently attracted significant attention in the storage and adsorption of gases, including in the separation of biogas to relatively pure streams of biomethane and biogenic CO_2 [34,146,147]. Fig. 5 illustrates the schematic operation of the PSA system in the CO_2/CH_4 gas separation with a typical packed MOF sorbent material.

Cavenati et al. [130] demonstrated that Cu-BTC MOF has a higher adsorption selectivity to CO_2 than CH_4 at a higher pressure of up to 40 bar. The study showed that at lower pressure (<5 bar), the selectivity to CO_2 adsorption is enhanced significantly. There is a correlation between CO_2 adsorption and low partial pressures, which is essential as low operating pressures are industrially desirable. In the other study, Chidambaram et al. [106] investigated the robustness of Al-PMOF and Al-PyrMOF in biogas upgrading in the presence of moisture. It was observed that due to the aromaticity of organic linkers, which conferred hydrophobicity to the MOFs, as well as the inertness of CH_4 and lack of quadrupole moment, the adsorption of CO_2 is higher in both MOFs at 293 K and 303 K. The adsorption of the gases at the latter temperature was decreased due to the increased thermal energy of the gases with elevated temperatures. Furthermore, Al-PMOF had a specific surface area and pore volume of 1244 m^2/g and 0.536 cm^3/g, respectively, whereas Al-PyrMOF exhibited 1109 m^2/g and 0.480 cm^3/g. Owing to the superior textural properties, Al-PMOF adsorbed more CO_2 (163.92 cm^3/g) than Al-PyrMOF (95.6 cm^3/g) at 2 bar and 303 K, respectively [106]. In addition, it was shown that due to the hydrophobicity of the ligands in the MOFs, the presence of moisture in a 50/46/4 vol% ($CO_2/CH_4/H_2O$) simulated biogas stream did not influence the CO_2 breakthrough curve where a breakthrough time of 11 min/g at 1 bar, 303 K, and 10 mL/min was maintained in both wet and dry conditions [106]. According to Karimi et al. [131], increased pressure and decreased temperature resulted in higher CO_2 adsorption of up to 4.5 mol/kg at 7–8 bar and 313 K. In contrast, a maximum of 3 mol/kg was adsorbed at 373 K under similar pressure conditions. A similar effect of pressure and temperature was observed for CH_4 and N_2 adsorption isotherms [148]. Furthermore, shaped MIL-160 (Al) was reported to have higher CO_2 adsorption than CH_4 and N_2, i.e., $CO_2 > CH_4 > N_2$, respectively. The isosteric heats of adsorption were the highest for CO_2 (−32 kJ/mol at a loading of 1 mol/kg) and lowest for N_2 (7 kJ/mol at less than 1 mol/kg loading). An increase in adsorption concentration resulted in a decrease in isosteric heat of adsorption for CO_2 and N_2, with an increase observed for CH_4. Furthermore, using the linear-driving-force (LDF) model, CO_2 uptake on shaped MIL-160 (Al) was found to increase with pressure and temperature, where an uptake (k_{LDF} value) of 0.021 s^{-1} was observed at 0.11 bar compared to 0.096 s^{-1} at 2.76 bar where both runs were performed at 313 K [148]. When the temperature was increased to 373 K, a CO_2 uptake of 0.584 s^{-1} at 2.8 bar was achieved. It was found that an increase in pressure promoted faster equilibrium adsorption. For example, 80 s at 0.11 bar and 35 s at 2.3 bar at 313 K, while the uptake equilibrium reached faster at 373 K (25 s). A similar effect of increased k_{LDF} values with temperature and pressure were observed for CH_4 uptake on shaped aluminium carboxylate MIL-160 (Al) MOF. However, the CH_4 uptake rates were higher than for CO_2. Furthermore, in the examined selectivity of MIL-160 (Al) for binary gas mixtures such as N_2/CO_2 and CH_4/CO_2 (50/50, v/v) at 313 K and 343 K, the N_2/CO_2 selectivity was found to be higher than for CH_4/CO_2 at 1.5 bar (18 vs. 4) [148]. Overall, it was concluded that for shaped MIL-160 (Al), the CO_2 adsorption equilibrium was higher than for CH_4 and N_2 at 313 K and 3.7 bar, respectively.

Functionalisation of MOF surfaces with amine groups bearing basic sites is one of the strategies that proved pivotal in improving the adsorption capacity [149–154]. This was demonstrated by Lin et al. [138] in testing the effect of amine functionalisation of MIL-101 (Cr) on CH_4, N_2, and CO_2 adsorption capacities at various temperatures and pressures. The study revealed that amine-functionalized MIL-101 (Cr) exhibits higher adsorption of CO_2 than N_2 and CH_4. The adsorption capacity of CO_2 was 15 mmol/g at 16 °C compared to about 5 mmol/g and <2 mmol/g for CH_4 and N_2, respectively. The superior CO_2 adsorption capacity was attributed to the Lewis basicity of the amine functional groups in MIL-101, facilitating stronger interaction with the acidic CO_2 molecule. The N_2/CO_2 selectivity was reported to be 8–16 and 3–5 for CH_4/CO_2 at 25 °C. The higher adsorption capacity for CH_4 compared to N_2 was ascribed to its relatively smaller molecular size. A slight decrease in the adsorption capacity of all the gas adsorbates when the temperature was increased from 0.4 °C to 25 °C was observed. In a separate study, Taheri et al. [139] investigated the effect of the synthesis time of MIL-53 (Al) and MIL-101 (Cr) hybrid composites for biogas upgrading. It was found that the CO_2 adsorption capacity of the MOFs was directly proportional to the surface areas where pristine MIL-53 (Al) and MIL-101 (Cr), with surface areas of 2254 and 1153.7 m^2/g, exhibited CO_2 adsorption capacities of 20 and 12 mmol/g, respectively. The hybrid MOF with the highest surface area of 1745.8 m^2/g had gravimetric CO_2 adsorption that was 35% more than MIL-53 (Al) but 20% less than MIL-101 (Cr) at 16 and 12 mmol/g at 40 bar. Furthermore, it was observed that for the adsorption of CH_4, an increase in the synthesis time of the hybrid MOF composites resulted in low pore diameters where the pores become smaller than the kinetic diameter of CH_4 (0.33 nm). As such, the authors observed that the CH_4 adsorption

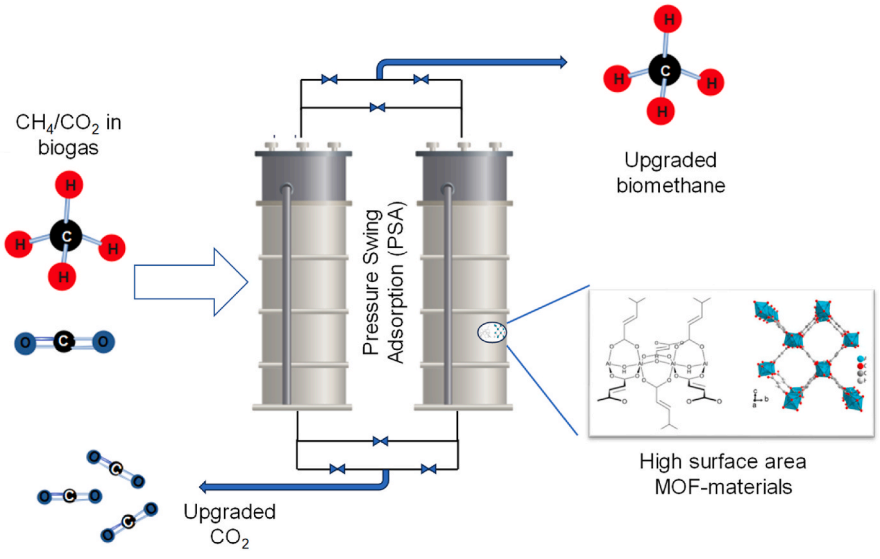

Fig. 5. Schematic illustration of biogas upgrading using a PSA unit packed with MOFs.

capacity did not follow a similar trend to CO_2, where an increase in surface area was not proportional to the adsorption capacity at ambient temperature and pressures of up to 40 bar. In addition, an Extended Langmuir (EL) model using a binary CO_2/CH_4 mixture at 298 K was applied. The EL model showed the hybrid MOF composite with the highest surface area to exhibit the most CO_2/CH_4 selectivity at 59.34. In contrast, pristine MIL-53 (Al) and MIL-101 (Cr) had a selectivity of 12.47 and 4.61, respectively. The high selectivity toward CO_2 in the hybrid MOF composite was attributed to the electrostatic field emanating from the pristine MOFs, such as the hydroxyl functional groups of MIL-53 (Al) and the MIL-101 (Cr) open metal sites. For instance, the polarity of CO_2 results in strong interactions with the hybrid MOF in addition to the size exclusion of CH_4. Indeed, the pore diameter of MOFs has a huge bearing on the size of gases that may diffuse in the cavities of the framework [155,156]. In a separate study, Mahdipoor et al. [157] investigated the effect of an amine-functionalized benzene dicarboxylate linker on MIL-101 (Fe) on the adsorption of CH_4, CO_2, and N_2 as well as the selectivity toward each molecule. The study revealed that due to the quadruple moment of CO_2 and the surface electric field of the anion of the amino-BDC, there was enhanced equilibrium adsorption at moderate temperature and pressure of up to 40 bar. For instance, increased CO_2 adsorption with pressure was observed up to 13 mmol/g, whereas 5 and 3.8 mmol/g adsorption of CH_4 and N_2 were reported. Furthermore, MIL-101 (Fe)–NH_2 exhibited higher selectivity to CO_2 over CH_4 and N_2, whereas, at pressures of 16.1 bar and 23.5 bar, the selectivity for CO_2 was found to be 2.21 and 6.46 for a CO_2/N_2 binary mixture [157]. For a CH_4/CO_2 mixture at 298 K with pressures of 16.8 and 27.9 bar, the selectivity was found to be 2.19 and 4.51, respectively. In addition, it was found that a hybrid of BET and Khan models resulted in a more acceptable correlation coefficient of the experimental data for CO_2 adsorption in comparison to the individual models. The beneficial effect of linker functionalisation on CO_2 adsorption capacity was further demonstrated by Chen et al. [158] in a study that compared pristine Zr-UiO-66 MOF against UiO-66-NH_2 (amide-functionalized BDC) and UiO-66-DAM (crosslinked amine-BDC). It was shown that linker functionalisation decreased the surface area of the MOFs. However, CO_2 adsorption was enhanced from 41.1 cm^3/g in the neat UiO-66 to 48 cm^3/g in UiO-66-NH_2 and 54.1 cm^3/g in UiO-66-DAM at 298 K and 1 bar. At lower pressure, the enhancement of CO_2 adsorption was found to be even more pronounced. This was because of the amide functionalisation of UiO-66, which resulted in stronger adsorption sites for CO_2 in the pores. The CH_4/CO_2 selectivity in a 50%/50% binary mixture between 0.1 and 1 bar pressure was higher for UiO-66-DAM, followed by UiO-66 and then UiO-66-NH_2. The high selectivity of UiO-66-DAM for CO_2 was ascribed to a strong dipole-quadrupole moment between the CO_2 adsorbate and the polar amide sites in the MOF sorbent material. As a result, the polarisable functional groups of UiO-66-DAM and UiO-66-NH_2 MOFs interacted strongly with the dipole moment of the C atom in CO_2, thereby resulting in higher isosteric heats of adsorption. In addition to the linkers, the oxygen in CO_2 binds strongly to open Zr(IV) metal sites in the clusters on the functionalized MOFs.

In addition to MOFs, zeolitic imidazolate frameworks (ZIFs) have also been explored for the capture of CO_2 mixed with various gases [159,160]. ZIFs are a class of crystalline and porous materials made from tetravalent transition metals such as Zn and Co bridged by imidazolate organic linkers, (Fig. 6) [161]. ZIFs, when compared to MOFs, have a higher CO_2 adsorption capacity, lower energy consumption, and high chemical and thermal stability [160]. The porosity of ZIF, especially ZIF-8, allows for the separation of CO_2 with a kinetic diameter of 3.4 Å from methane. It has been reported that CO_2 diffuses two times faster

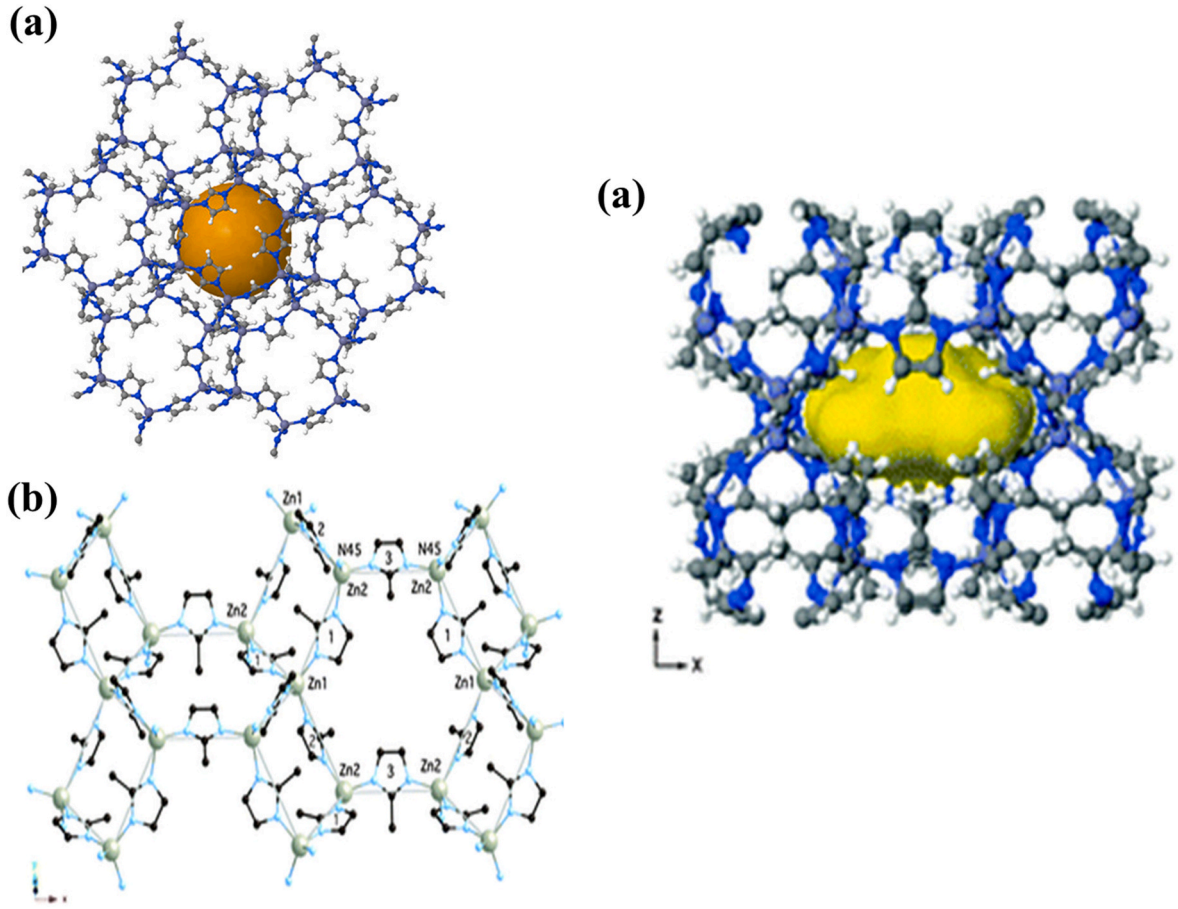

Fig. 6. Structures of (a) ZIF-8, (b) ZIF-L, and (c) their pore geometry. Reprinted from Ref. [4].

than CH_4 in ZIFs, making them suitable for upgrading biogas [162]. Similarly to MOFs, the structure of ZIFs can be functionalized to increase CO_2 adsorption capacity. Abdelhamin, for instance, investigated the effects of different salts (NaCl, KNO_3, K_2CO_3, and HCOONa) as modulators in the synthesis of ZIF-8 on CO_2 adsorption [163]. The study reported Type I CO_2 adsorption isotherms when using the modulators. Furthermore, the CO_2 adsorption capacity increased from 0.80 to 0.99 mmol/g in ZIF-8 (NaOH) and ZIF-L (NaOH), Table 4. The increase in CO_2 adsorption was attributed to the residual cations in the framework of ZIF-8 due to their electrostatic interactions with CO_2. In addition, the van der Waals forces of ZIF-8 enhance CO_2 adsorption [164]. The synthesis of ZIF-8 may also be modulated using a cellulose derivative such as 2,2,6,6-tetramethylpiperidine-1-oxyradical (TEMPO)-mediated oxidised nanocellulose (TEMPO) where Abdelhamin et al. reported CO_2 adsorption capacities of CelloZIF-8 of 0.33–0.57 mmol/g and 0.58–1.1 for CelloZIF-L (A two-dimensional derivative of ZIF-8) [164]. The modulated synthesis improves the results in higher pore volumes, allowing CO_2 adsorption at high pressure [164]. In addition, hybrid materials with ZIFs can improve separation from various gas mixtures [165]. Alrich et al., for instance, investigated the CO_2/CH_4 selectivity of zeolite 4A and ZIF-95 composites (Zeolite@ZIF-95), Fig. 7 [166]. The study highlighted that the zeolite@ZIF-95 composite, compared to the pristine material, had a lower heat of adsorption. Furthermore, the zeolite@ZIF-95 composite had higher CO_2 adsorption than CH_4 at 273 K and 298 K due to the suitable pore diameter and interaction of CO_2 with the imidazolate ligands in the framework. Due to the suitable adsorption capabilities, ZIFs are a viable alternative to MOFs for biogas upgrading [167]. In a separate study, Bai et al. prepared N-doped carbon material derived from the carbonisation of ZIF-8 [168]. At 1 bar and 25 °C, pristine ZIF-8 had a CO_2 adsorption capacity of 0.31 mmol/g compared to 3.8 mmol/g N-doped ZIF-derived carbons. The difference in CO_2 adsorption capacity was attributed to the small pore mouth of ZIF-8 used in the study and the high surface area of the N-doped carbon.

6. MOF-graphene oxide (MOF-GO) composites for CO_2 adsorption

MOFs can be functionalized to make composites tailored to enhance CO_2 separation from various gas streams [182,183]. For instance, Zhao et al. prepared MOF-5-H (Prepared in a homogenous reactor), and their graphene oxide composites: MOF-5-H with graphene oxide (MOF-5--GO-H), MOF-5-O with aminated graphene oxide prepared in a drying oven (MOF-5-AGO-O) [184]. The CO_2 adsorption capacity at 298K and 4 bar were reported to be 0.64 mmol/g (MOF-5-H), 0.54 mmol/g (MOF-5-AGO-O), and 1.06 mmol/g (MOF-5-GO-H). The latter was found to have higher CO_2 adsorption than pristine MOF-5-H and the amine-functionalized counterpart, MOF-5-AGO-O. The relatively high CO_2 adsorption of MOF-5-GO-H was attributed to the surface area of 409 m^2/g and pore diameter of 0.409 nm, similar to the kinetic diameter of CO_2. In contrast, the pristine MOF-5-H had a pore diameter of 0.550 nm. The study reported that MOF-composites with a pore diameter close to the kinetic diameter of CO_2 enhance adsorption and, therefore, separation from various gas streams. The CO_2 adsorption of the amine-functionalized graphene oxide and MOF-5-O composite (MOF-5-AGO-O) was higher than that of pristine MOF-5-H at pressures lower than 1 bar. The higher adsorption was attributed to the nitrogen-containing amino groups, which offer better interactions with the CO_2 adsorbate. However, due to the limited number of amino groups, there is relatively quick saturation of the adsorption sites, which results in low CO_2 adsorption at pressures higher than 1 bar. Zhao et al. also investigated composites of amine-functionalized GO and Cu-BTC MOF [185]. The authors used urea at concentrations of 0.030, 0.150, and 0.300 mol/L to functionalise GO to GO-U1, GO-U2, and GO-U3. The MOF-GO composites MOF/GO-U1, MOF/GO-U2, and MOF/GO-U3 had CO_2 adsorption capacities of 4.23, 2.76, and 2.02 mmol/g at 303 K and 1 bar. The CO_2 uptake of the amine-functionalized GO/MOF composites

Table 4
Summary of some MOFs' properties related to porous materials and their performances in CO_2 adsorption capacity.

MOFs name	Synthesis method	BET surface area (m^2/g) and pore volume (cm^3/g)	CO_2 adsorption	Ref
IRMOF-3	Solvothermal	981.43 m^2/g and 0.5 cm^3/g	1.39 mmol/g	[169]
AMP@IRMOF-3 (75 wt%)	Solvothermal	962.57 m^2/g and 0.39 cm^3/g	3.9 mmol/g	
IRMOF-11	Solvothermal	2096 m^2/g	13 mmol/g	[170]
UiO-66 DAM	Solvothermal	651 m^2/g and 0.3 cm^3/g	[a] 54.1 cm^3/g	[171]
UiO-66(Zr)	Sol-gel reflux	425.32 m^2/g	[b] 428.7 cm^3/g	[172]
NH_2-MIL-53(Al)	Solvothermal	212 m^2/g	1.89 mmol/g	[173]
MOF-177	Solvothermal	4508 m^2/g	33.5 mmol/g	[170]
MOF-74(Ni)-cordierite monolith	Solvothermal	652 m^2/g and 0.73 cm^3/g	1.7 mmol/g	[174]
meso-HKUST-1	Hydrothermal	1462 m^2/g	7 mmol/g	[175]
HKSUT-1		1334 m^2/g	6 mmol/g	[175]
Al-PM	Solvothermal	1244 m^2/g and 0.536 cm^3/g	[c] 163.92 cm^3/g	[106]
Al-PyrMOF		1109 m^2/g and 0.480 cm^3/g	[c] 95.6 cm^3/g	[106]
Cu-PSB	Solvothermal	651 m^2/g and 0.3 cm^3/g	4.8 mmol/g	[176]
UTSA(University of Texas at San Antonio)-16(Co)	Solvothermal	746 m^2/g and 0.36 cm^3/g	3.79 mmol/g	[101]
UTSA-16(Co)-cordierite monolith		223 m^2/g and 0.11 cm^3/g	1.1 mmol/g	[101]
Ni-DABCO	Solvothermal	2120 m^2/g and 0.82 cm^3/g	2.17 mmol/g	[177]
Zn-DABCO		1870 m^2/g and 0.69 cm^3/g	1.87 mmol/g	[177]
MOF 210		6240 m^2/g and 3.6 cm^3/g	[d] 2870 mg/g	[178]
MIL-101 (Cr)–NH_2	Hydrothermal	1675 m^2/g	15 mmol/g	[179]
MIL-101 (Cr)	Hydrothermal	2254 m^2/g and 1.18 cm^3/g	20 mmol/g	[180]
MIL-53 (Al)		1153.7 m^2/g and 0.55 cm^3/g	12 mmol/g	
MIL-101(Cr)@MIL-53 (Al)		1745.8 m^2/g and 0.52 cm^3/g	16 mmol/g	
MIL-101 (Fe)–NH_2	Solvothermal	915 m^2/g	13 mmol/g	[157]
Amino-MIL-53 (Al)	Solvothermal	–	6.7 mmol/g	[181]
ZIF-8 (NaOH)	Hydrothermal	1300 m^2/g and 0.56 cm^3/g	0.8 mmol/g	[163]
ZIF-8 (NaOH + NaCl)		1620 m^2/g and 0.78 cm^3/g	0.85 mmol/g	
ZIF-8 (NaOH + KNO_3)		1390 m^2/g and 0.6 cm^3/g	1.02 mmol/g	
2D ZIF-8 (NaOH)		–	1.05 mmol/g	
2D ZIF-8 (NaOH + NaCl)		–	0.99 mmol/g	

[a] T = 298 K, P = 1 bar.
[b] T = 273 K, P = 1 bar.
[c] T = 303 K, P = 2 bar.
[d] T = 298 K, P = 50 bar.

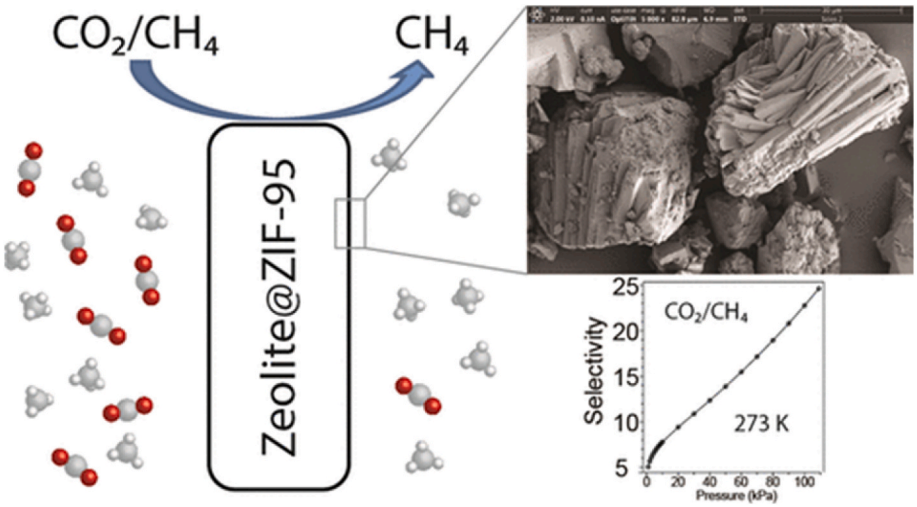

Fig. 7. Zeolite@ZIF-95 composite for CH_4/CO_2 separation. Reprinted from Ref. [166].

was higher than that of the pristine MOF (2.00 mmol/g). Therefore, it was proposed that the nitrogen content in the composites enhances CO_2 adsorption via reactions 1 and 2, where CO_2 reacts with $–NH_2$ groups of the amino groups [186,187]. The latter and the π-electron delocalisation of the GO aromatic groups favour the physisorption of CO_2 via the quadrupole moment, which is a more robust interaction than van der Waals forces [31]. The schematic of the Cu-BTC/GO-U composites is shown in Fig. 8.

$$-NH_2 + CO_2 \leftrightarrow NH_2^+COO^- \quad (1)$$

$$-NH_2 + NH_2^+COO^- \leftrightarrow NHCOO^- + -NH_3^+ \quad (2)$$

In a separate study, Chen et al. investigated various loadings of graphene oxide on MOF-505 for the separation of CO_2/CH_4 and CO_2/N_2 [32]. Four MOF-505@GO composites were prepared with GO loading of 2, 5, 8, and 10 wt%, i.e. MOF-505@2GO, MOF-505@5GO, MOF-505@8GO, and MOF-505@10GO. At 1 bar and 298K, the pristine MOF-505 had CO_2 adsorption of 2.87 mmol/g, whereas pristine GO did not show any CO_2 adsorption capacity. The MOF-505@GO composites were found to have higher CO_2 uptake than the pristine MOF-505 and GO, where MOF-505@2GO and MOF-505@5GO had CO_2 uptakes of 3.46 mmol/g and 3.94 mmol/g. The superior CO_2 adsorption of the composites was attributed to dispersive forces on the surface, high surface area, and a surface defect resulting from coordinatively unsaturated Cu^{2+} metal sites in the parent MOF [188,189]. Furthermore, the study reported that the CH_4 and N_2 adsorption capacities of the parent material and their composite counterparts were significantly lower than that of CO_2, where less than 1 mmol/g of CH_4 and less than 0.3 mmol/g of N_2 across all the materials. The difference in adsorption capacity was reported due to the lack of adsorption sites for CH_4 and N_2, highlighting the high selectivity toward CO_2. The benefit of MOF-GO composites on CO_2 adsorption was also reported by Cao et al. [190], where zirconium-based MOF, UiO-66, was used to make composites with 1%, 5%, and 10% GO, i.e., UiO-66/GO-1, UiO-66/GO-5, and UiO-66/GO-10. Pristine UiO-66 had a CO_2 adsorption capacity of 2.27 mmol/g at 1 bar and 298 K compared to the UiO-66/GO-5 composite at 3.37 mmol/g. The composite with the highest GO content, UiO-66/GO-10, had a CO_2 adsorption capacity lower than UiO-66/GO-5, which was due to pore filling in the UiO-66 MOF by GO, thereby decreasing the available pore volume for CO_2 adsorption. Indeed, various MOF/GO composites have been reported to have superior CO_2 uptake compared to the pristine MOF and GO material [191]. Furthermore, the amino functional groups in GO, coordinatively unsaturated sites, and the delocalisation of electrons interact strongly with the quadruple moment of CO_2, which results in better adsorption [192].

7. Pure MOF membranes for biogas cleaning

Pure MOF membranes have been explored as potential alternatives to membrane technologies for removing contaminants from waste

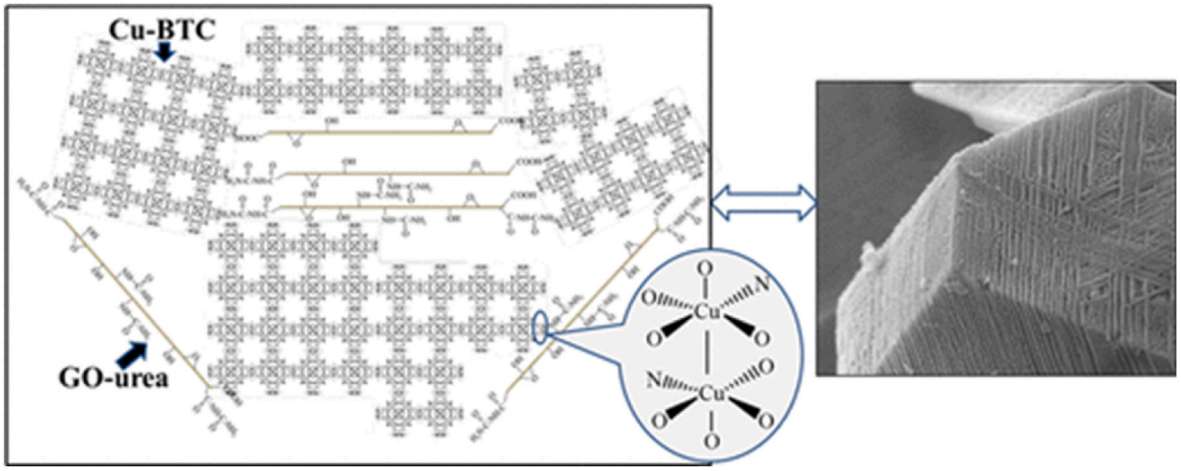

Fig. 8. Diagram of amine-functionalized Cu-BTC/GO composites. Reproduced from Ref. [185].

streams owing to their high porosity and customisable pore chemistry. Only some studies have reported on using pure MOF membranes for pollutant removal from various gas streams with success and failure. In most cases, failures were attributable to the frame flexibility [193] or structure defects [194] that could cause expanded pore aperture size and provide comparable opportunities for the second species in the gas mixtures to pass through, leading to competitive diffusion and decreased selectivity. Therefore, membrane stability is a vital aspect affecting membrane performance. It has been noted that most MOF membrane research focused on zeolitic imidazolate framework (ZIF) due to their impressive separation properties, ease of synthesis, and the feasibility of forming high-quality membranes [195]. Bux et al. [195] synthesised the first ZIF 8 membranes and demonstrated their performance for hydrogen purification. Subsequently, Pan et al. [196] developed a 2 μm thick ZIF-8 membrane on the shell side of yttria-stabilized zirconia (YSZ) hollow fibre. They demonstrated its application for H_2/C_3H_8 separation, achieving a high H_2 permeance of 5077 GPU and an H_2/C_3H_8 ideal selectivity of 500. A different study successfully synthesised the ZIF 62 MOF glass membrane by melt-quenching it on alumina support and utilising it as a membrane material [197]. The material was evaluated for separation of H_2/CH_4, CO_2/N_2 and CO_2/CH_4 mixtures, resulting in 50.7, 34.5, and 36.6 separation factors, far exceeding the Robeson upper bounds. Nguyen et al. [181] demonstrated that high-quality separation membranes typically exhibit permeance of over 5000 GPUs and high gas selectivity based on the separation factor. The study by Chiou et al. [198] emphasised the scarcity of MOF membranes that meet the selectivity threshold necessary for industrial applications, which typically requires a selectivity value exceeding 30. Literature concerning using pure MOF membranes for biogas cleaning and upgrading is scarce. However, several studies have explored the potential of MOF membranes for separating individual constituents commonly found in biogas. Table 5 presents the summary of some of the studied pure MOF membranes.

Pure MOF membranes have generally demonstrated superior gas separation performance to conventional zeolite and polymer membranes, exhibiting higher separation factors and permeabilities. However, their widespread application has been hindered by the difficulties involved in their fabrication, including problems such as framework flexibility, defects, and grain orientation. Framework flexibility allows larger molecules to pass through, while defects in the membrane act as non-selective pores, potentially allowing molecules of various sizes to pass through, which can affect the overall separation performance of membranes. Some must show the expected gas permeation behaviour, making them expensive alternatives. Consequently, researchers have sought alternative strategies to overcome these challenges, such as developing mixed-matrix membranes by incorporating MOFs into easily processable polymers.

8. MOFs with mixed-matrix membranes for biogas cleaning

Membrane technologies have been successfully adopted in gas separation processes, including upgrading biogas [208]. While they hold significant promise, they are masked by substantial setbacks, particularly in gas permeability, which results in low fluxes and selectivity, thus

Table 5
Summary of the biogas-related gas separation results of the different MOF membranes.

MOF membrane	Support	Membrane thickness (μm)	Gas stream mixture	Performance	Ref
ZIF-8 membrane	Supported on stainless steel nets	4.9	H_2/CO_2	H_2 permeance: 7×10^{-6} mol/m^2 s Pa H_2 separation factor: 11.3	[199]
ZIF 8	Supported on polydopamine functionalized macroporous stainless-steel-nets.	30	H_2/CO_2 H_2/N_2 H_2/CH_4 H_2/C_3H_8 binary mixtures	H_2 permeance: 2.1×10^{-5} mol/m^2 s Pa Separation factor: H_2/CO_2: 8.1 H_2/N_2: 15 H_2/CH_4: 23.2 H_2/C_3H_8: 329.7	[200]
CAU-10-H MOF membrane	Porous alumina substrate	4–5	CO_2/CH_4 CO_2/N_2	CO_2 permeance: 1.7×10^{-13} mol m^{-2} s^{-1} Pa^{-1} ideal selectivity for CO_2/N_2:42 CO_2/CH_4:95	[198]
ZIF 8 membrane	Tubular alumina (α-Al_2O_3) supports	~5–9	CO_2/CH_4 mixture	CO2 permeance: ~2.4×10^{-5} mol/m^2 s Pa CO_2/CH_4 selectivities from ~4 to 7	[201]
Pure ZIF 67 membrane	Tubular substrate	1.7	H_2/N_2 H_2/CH_4	H_2 permeance of 5.59×10^{-7} mol m^{-2} s^{-1} Pa^{-1}. ideal separation factors for H_2/N_2 and H_2/CH_4 are 14.7 and 15.3, respectively.	[202]
ZIF 67 membranes	Supported on ZnO hollow fibres	13.8	H_2/N_2 H_2/CO_2 H_2/CH_4 binary mixtures	H_2 permeance was 8.98×10^{-8} mol m^{-2} s^{-1} Pa^{-1}. Ideal selectivities for H_2 gas pairs with CO_2, N_2, and CH_4 were 5.14, 11.75, and 15.89, respectively	[203]
ZIF 8	Ceramic hollow fiber	150	H_2/CH_4 H_2/C_3H_8	H_2 permeance: ~15×10^{-7} mol/m^2 s Pa. Ideal selectivity: ~13 Separation factor: 10 7.1×10^{-7} mol/m^2 s Pa. Ideal selectivity: 1100 Separation factor: 474	[204]
ZIF 7	Asymmetric alumina disks	1–2	H_2/N_2	H_2 permeance: 8×10^{-8} mol m^{-2} s $^{-1}$Pa^{-1} H_2/N_2 separation factor: 7.7	[205]
ZIF-8	Polyvinylidene fluoride hollow fibres	1.2	H_2/CO_2 H_2/N_2 H_2/CH_4 H_2/C_3H_6 H_2/C_3H_8 binary mixtures	H_2 permeance: 1.6×10^{-6} Ideal selectivity: H_2/CO_2: 6 H_2/N_2: 10.2 H_2/CH_4: 12.1 H_2/C_3H_6: 56.6 H_2/C_3H_8: 160.1	[206]
IRMOF-1	α-Al_2O_3 support		CO_2/CH_4 CO_2/N_2	CO_2 permeance of 2.55×10^{-7} Separation factor: 328 CO_2 permeance of 2.06×10^{-7} mol m^{-2} s^{-1} Pa^{-1} Separation factor: 410	[207]

(1 GPU = 3.349×10^{-10} mol/m^2 s Pa).

hindering their application on an industrial scale [209]. The low flux in membranes usually demands large membrane surface areas, which entails high capital costs. Meanwhile, low selectivity leads to elevated operating costs due to the energy-intensive multistage separation processes necessary to mitigate selectivity limitations. Further challenges include penetrant-induced plasticisation, physical ageing, conditioning, and the delicate equilibrium between permeability and selectivity, which some have an effect on CO_2 induced plasticisation in industrial applications for natural gas processing [210]. Fig. 9a depicts summarised critical factors of MOFs, as Fajrina et al. reported [211]. Further, Fig. 9b presents a schematic diagram comparing the biogas cleaning performance of pristine MOFs, polymer membranes, and MOF-based membranes such as mixed-matrix membranes (MMMs) for gas separation and purification. The percentage impurities removal values indicated in Fig. 9b are used purely for illustrative purposes to show the benefits of incorporating MOFs in the membrane system, derived from deductions drawn from numerous research studies documented in the literature, as summarised below in this section discussion. Furthermore, Table 6 provides a summary of some reported MOFs and membrane integrated MMM systems that are promising for the removal of different trace biogas impurities and the upgrade of CH_4/CO_2. They demonstrated the potential for developing an integrated one-material/membrane MMM composite to achieve excellent efficiencies for biogas trace impurities removal simultaneously with CH_4/CO_2 upgrade as one operated entity, one unit, or stage.

As an example, a neat polymer-based membrane on acrylonitrile-butadiene-styrene/poly (vinyl acetate) for CO_2 removal with more excellent selectivity for CO_2 over N_2 in the CO_2/N_2 mixture compared to CO_2/CH_4 separation due to variations in molecular sizes and polarities of the gases involved was demonstrated [223]. However, the performance of this polymer membrane suffered deterioration rapidly because of structural stability. Further, two polymer-based materials of PA12-PEO-50 and PA6-PEO-60 membranes were assessed for their gas permeability and selectivity across diverse conditions, encompassing pure and mixed gases [224]. A deterioration in performance was observed as the testing conditions shifted from pure gas permeation to 20% mixed gas permeation. These highlighted membrane problems, including their low surface areas, have recently ignited considerable interest in exploring diverse filler materials, including zeolites and graphene nanosheets, to mitigate compatibility issues and enhance membrane selectivity and permeability while maintaining excellent mechanical strength and ease of processing. Recently, MOFs have emerged as attractive fillers in MMM composite technologies for gas separation, including biogas cleaning and upgrade, due to their unique physicochemical properties [225–228]. The advantages of MOF-based integrated MMMs compared to neat MOF sorbent or membranes include enhanced selectivity, increased gas permeability, reduced energy consumption, scalability, customizability, and the potential for hybrid synergy [35,229].

MOFs based on UiO-66 and its functionalized NH_2-UiO-66 were immobilised into a polyether block amide (PEBA) membrane to construct MMM to separate CO_2 (Fig. 10a–c). The functionalized NH_2-UiO-66 showed a stronger affinity for CO_2 than neat UiO-66 in their respective MMM composites driven by suitable hydrogen bonding structure framework interactions between PEBA and NH_2-UiO-66, leading to improved polymer matrix dispersity. Both the UiO-66-PEBA and NH_2-UiO-66-PEBA MMMs demonstrated higher performance for CO_2 separation compared to neat PEBA membrane or individual NH_2-UiO-66 and UiO-66 MOFs (Fig. 10c). The NH_2-UiO-66-PEBA obtained better separation selectivity for N_2/CO_2 and slightly reduced CO_2 permeability compared to those of non-amine functionalized UiO-66-PEBA membrane. Even in humid conditions, the NH_2-UiO-66-PEBA

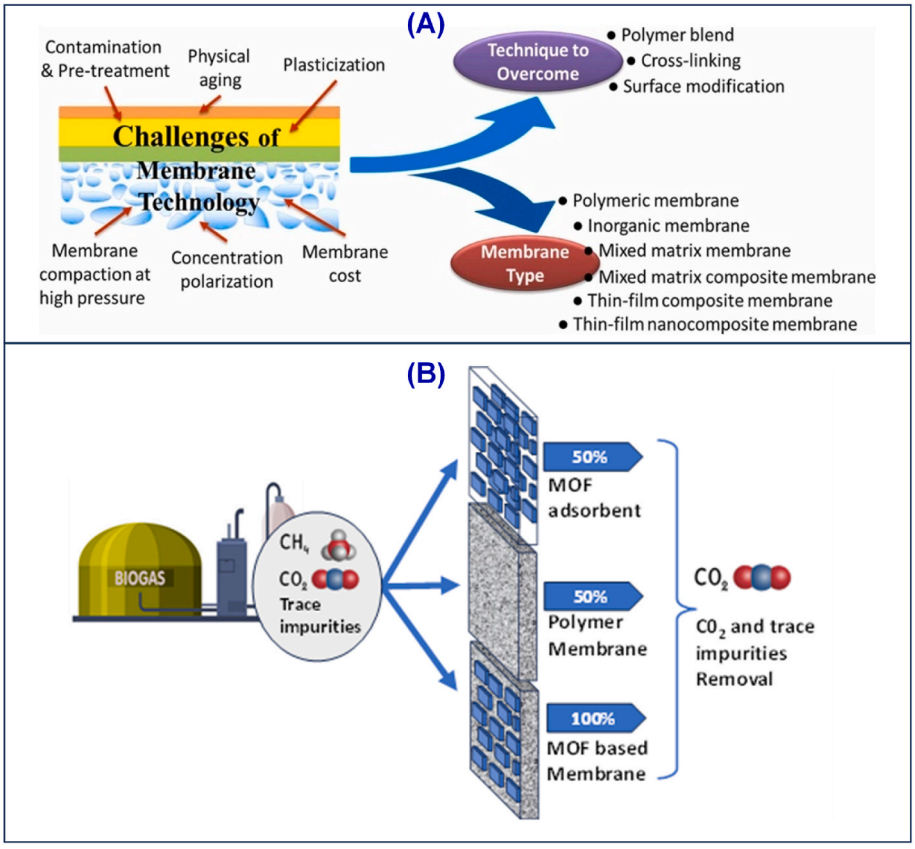

Fig. 9. **(a)** Summary of membrane technology for gas separation highlighting challenges and potential strategies to overcome them. Reprinted from Ref. [211]. **(b)** Illustration of the typical biogas cleaning performance of pristine, polymer, and MOF-based membranes.

Table 6
Summary of some MOFs and MMMs composites for biogas cleaning and upgrade.

MOF based membrane	Gas mixture	Comments on performance	Ref
Fluorinated MOF-based membrane	H_2S CO_2 CH_4	Fluorination of MMM enhanced its surface molecular-sieving properties for better performance compared to neat membranes in the simultaneous removal of H_2S and CO_2 upgrading from natural gas.	[212]
PPOP-COOH/UiO-66 (Zr)-$(COOH)_2$	H_2S CH_4	Enhanced performance for H_2S removal for MOF filler addition in the MMM to achieve increased high H_2S permeability and permeation selectivity.	[213]
Fluorinated AlFFIVE-1-Ni (KAUST-8)-Polymer membrane	H_2S	Enhanced separation efficiencies of the mixture of $H_2S/CO_2/CH_4$ (1/9/90) with better permeability for ($H_2S + CO_2$) of 63, 104, and 140% and improved ($H_2S + CO_2$)/CH_4 selectivity of 123, 112, and 103% promoted by MOF filler addition in various designed MMMs.	[214]
UiO-66-NH_2-embedded membranes	NH_3	Amine-modified NH_2-UiO-66 incorporation designed a high-performance MMM system with improved removal performance of NH_3 at transfer flux >9 g/m^2h and up to 90% efficiencies.	[215]
HKUST-1 MMM	NH_3	The performance of 30-HKUST-1 filled MMM for over 28 days was very stable, maintaining a higher NH_3 removal capacity than the pristine HKUST-1, with only 30 wt % loading of 30-HKUST-1.	[216]
10 wt% Alf-MOF fabricated into PVA layer	NH_3	PVA-modified MOF filler for various PFOS, PFHxS, and PTFE membranes showed substantial improvement in their removal NH_3 efficiencies, ranging from 65 to 99% depending on the MOF filler loading amounts. Incorporating PVP-MOF filler modified the membranes' hydrophilic properties, improving their removal activity performances.	[217]
UiO-66-NH_2 MOF PTFE membrane	NH_3	We achieved improved NH_3 capacity for filler-incorporated MOF in the GMM membrane of up to 1.13 mol/kg compared to typical values of MOF of 2.6 mol/kg for a packed bed of MOF pellets.	[218]
NH_2-MIL-125(Ti)/PSF	CO_2/CH_4	The PSF-NH_2-MIL-125(Ti) mixed matrix membranes (MMMs) demonstrated significant improvements in gas separation performance compared to pristine polymer membranes. The CO_2 separation factor increased from 22 to 29.2, while the permeability rose from 9.5 to 40 as the MOF filler loading escalated from 0 to 30 wt% in the MMMs.	[219]
ZIF-90/6FDA-DAM	CO_2/CH_4	Incorporating 15 wt% of ZIF-90A into a pure 6FDA-DAM membrane enhanced the CO_2 permeability (barrer) and selectivity from 390 to 720 and 24 to 34, respectively.	[220]
NH_2-MIL-53(Al)/PSF	CO_2/CH_4	For loadings up to 25 wt%, the addition of NH_2-MIL-53(Al) produces a moderate CO_2 flow increase and a slight decrease in CH_4 permeation that boosts CO_2/CH_4 membrane selectivity by two-fold for the best-performing membrane (25 wt%).	[221]
Matrimid 9725/MIL-125(Ti)	CO_2/CH_4	A significant increase in mixed gas selectivity and permeability of the membrane filled with NH_2-MIL-125 indicates that it is a perfect candidate for CO_2:CH_4 separations where highly permeable and selective membranes are required. An optimal selectivity of 50 was already reached at 15 wt% MOF loading, while higher loadings further increased permeability substantially.	[222]

with 10 wt% MOF loading maintained its stability for N_2/CO_2 separation performance at 130 Barrer CO_2 permeability and 72 selectivity of N_2/CO_2, which surpassed the standardised upper bound of polymer membranes (i.e., Robeson upper bound, 2008) (Fig. 10c). Another example of amine-functionalized MOF of different class, NH_2-MIL-125(Ti) (Fig. 11a), as a filler to construct polysulfone-based based MMM has been demonstrated for CH_4/CO_2 gases separation. The incorporated NH_2-MIL-125(Ti) platelets-like particles (Fig. 11b SEM) in the polysulfone-based MMM significantly enhanced the CO_2 permeability with a slight increase in CH_4/CO_2 separation factor compared to the neat polymer membrane (Fig. 11c and d) [219], The separation factor of NH_2-MIL-125(Ti)/polysulfone MMM remained unchanged at elevated pressures, which indicates that MOF-containing MMMs are promising for biogas CO_2/CH_4 upgrading.

In the other study taking advantage of 2D nanosheets morphology of MOF based on Co-benzenedicarboxylate (CBMN), a layered MMM composite combining CBMN filler interfaced with a carboxyl-functionalized polyimide (6FDA-durene-DABA) membrane for CO_2/CH_4 separation (Fig. 12). Benefiting from the high aspect ratio (>1000) of CBMNs, an intense interfacial contact with 2D MOF coordination bonds between the –COOH group of 6FDA-durene-DABA and Co^{2+} in CBMNs was formed that led to MMM with an improved separation performance of CH_4/CO_2 affected by CBMN loadings (Fig. 12a) and ideal CH_4/CO_2 selectivity of 33.6 ± 3.0 which surpassed the 2008 Robeson upper bound (Fig. 12b). The authors also demonstrated an enhanced CO_2 plasticisation pressure of the MMMs of up to ~20 bar, which was 2-fold higher compared to that of the neat 6FDA-durene-DABA membrane (Fig. 12c). The MMM based on 6FDA-durene-DABA/CBMN (2 wt %) demonstrated high stability for separation of mixed CO_2/CH_4, gases with selectivity maintained at around 23 and the CO_2 permeability kept around 400 barrer over 100 h operational testing period (Fig. 12d).

An MMM system containing $Zn(Pyrz)_2(SiF_6)$ (or SIFSIX-3-Zn) MOF and crosslinked polyethylene oxide polymer matrix membrane has been constructed for the separation of biogas CH_4/CO_2 and N_2/CO_2 mixtures (Fig. 13a) [235]. The fabricated MMM improved CH_4/CO_2 and N_2/CO_2 mixture's gas permeation and selectivity for CO_2 over CH_4 and N_2 compared to the neat MOF or membrane, respectively. The improved efficiency in gas separation was attributed to the enhanced MOF filler/polymer membrane interfacial voids created in MMM to promote selective and CO_2 uptake [235]. Further studies demonstrated the same trend of improved overall performance concerning high permeation and selectivity in the separation of CO_2/CH_4 gas mixture using MOFs filler-based MMMs of ZIF-90 nanoparticles embedded on three different poly(imide)s (Ultem, Matrmid, and 6FDA-DAM ZIF-90/6FDA-DAM) (Fig. 13b) and MOF-74 on PIM-1 (i.e. polymer of intrinsic microporosity with rigid and contorted polymer chain) (Fig. 13c) [236,237]. Apart from the design of MMMs using single MOF filler type, the recently

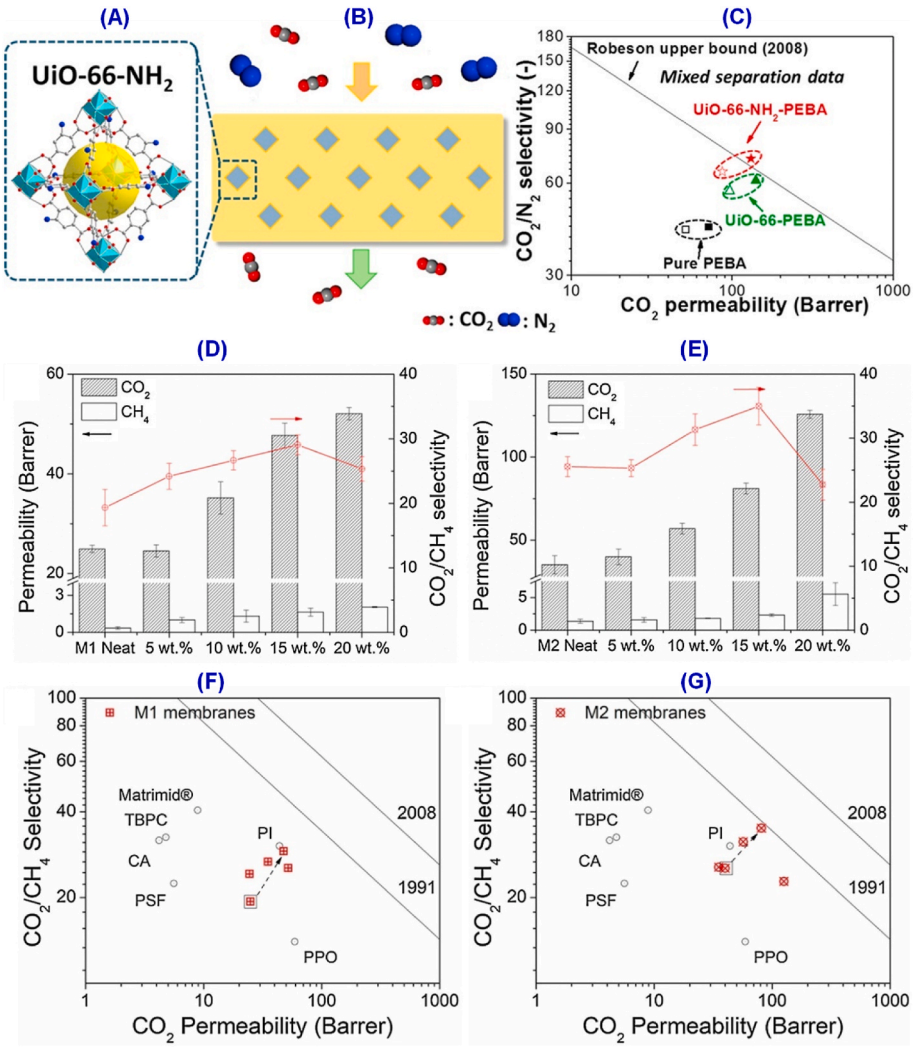

Fig. 10. (a) Neat UiO-66-NH_2; (b) UiO-66-NH_2/PEBA MMM, and (c) Mixed CO_2/N_2 gases separation performance of UiO-66-NH_2/PEBA MMM. Ref. [230]. (d)–(e) CH_4 and CO_2permeabilities, and CH_4/CO_2 selectivity of 6FDA-bisP and its ZIF-8 MMM. (f)–(g) Comparison of 6FDA-bisP and its M1 and M2 MMMs with standard 1991 [231] and 2008 [232] Robeson's plot. Ref. [233].

emerging trend of using composites of different interfaced MOFs as fillers to develop MMMs is attractive, with highly improved properties and performance. An improvement in higher selectivity and permeation for separation of CO_2/CH_4 gas mixture was obtained by combining a polysulfone (PSF) based MMM incorporated with 16 wt.-% loading of ZIF-8/MIL-101(Cr) mixed MOFs composites at 1:1 ratio (Fig. 13d) [220]. The mixed ZIF-8/MIL-101(Cr) integrated MMM performed better than the MMMs based on analogous single-filler ZIF-8 or MIL-101(Cr) MOFs.

Recently, ZIFs have gained significant interest in MOF-based membranes due to their excellent hydrophobicity, porosity, and high chemical and thermal stability [238]. This was demonstrated in the study that investigated the moisture stability of MOFs such as ZIF-8, the combination of ZIF-8 and ZIF-67 (ZIF-8/ZIF67), UiO-66 and their hybrid structures of appropriate functional groups and 2D nanosheets morphology interfaced with polymers membranes of high intrinsic permeabilities for potential application in biogas upgrading with excellent efficiencies [48,239]. For example, a poly (amide-*b*-ethylene oxide) (Pebax®1657, Arkema) mixed with the nanosized ZIF-7 MOF achieved higher performance for CO_2 separation from CH_4 and other gas streams better than virgin Pebax®1657 membrane [240]. A ZIF-7 MOF incorporated as the filler to develop a thin Pebax 1657-based MMM on PAN support achieved an optimal performance at a 34 wt% loading of ZIF-7. Further, the ZIF-7/Pebax 1657-based MMM/PAN composite exhibited a CO_2 permeance of 39 GPU along with N_2/CO_2 and CH_4/CO_2 selectivities of 105 and 44, respectively [240]. In the other study, the addition of MOF fillers in the Pebax® polymeric phase membrane promoted an improvement in the gas separation performance, especially in terms of permeance where the MMM containing a 10 wt% loading of UiO-66 MOF reached the optimum value of 11.5 GPU of CO_2 (together with a CH_4/CO_2 selectivity of 55.6) [241]. Xu et al. [190] enhanced the permeation performance of polyether-polyamide block copolymer membranes by incorporating ZIF-8 MOF nanocrystals that resulted in an increase in the CO_2 permeability from 79.2 to 156 Barrer as the ZIF-8 loading increased from 0 to 20 wt%. A similar trend of improvement was observed in the different studies involving the incorporation of 5 wt % of ZIF-8-9 in the MMM that achieved the optimal separation performance compared to the neat membrane [242]. This configuration showed a CO_2 permeability of 99.7 Barrer and N_2/CO_2 selectivity of 59.6, with both values highlighting a substantial increase of approximately 25% compared to the pure Pebax membrane [242]. Chiou et al. [243] developed a MOF membrane (CAU-10-H) for CH_4/CO_2 separation by leveraging the advantageous coulombic effect with aluminium hydroxide isophthalate MOF to achieve high CO_2 selectivity. Notably, the CAU-10-H MMM system exhibited a CO_2/CH_4 and N_2/CO_2 selectivity surpassing 30. Ordonez et al. [244] reported 4 times higher ideal

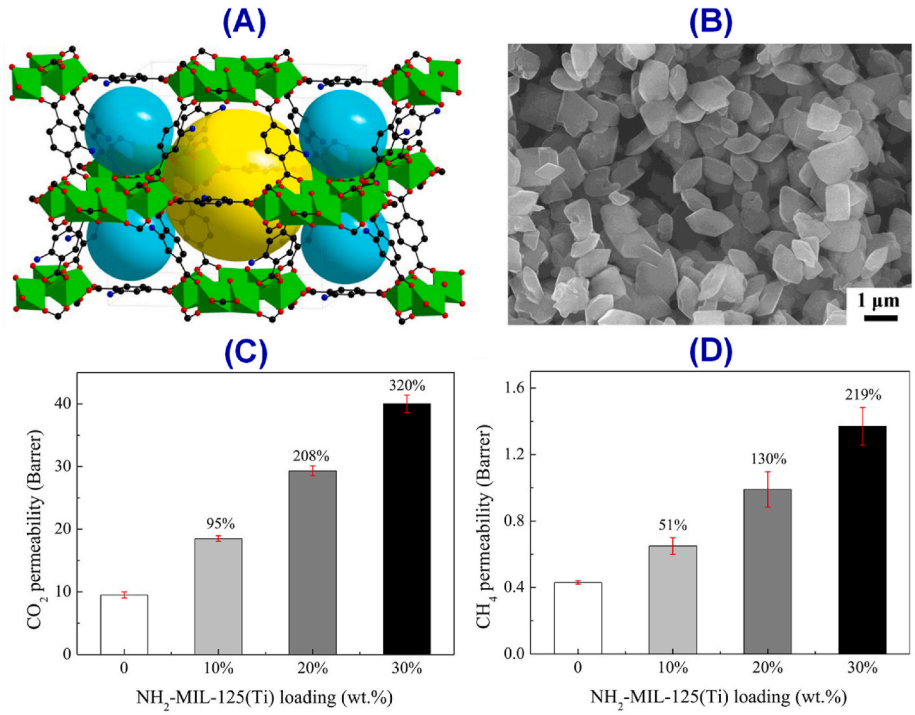

Fig. 11. (a) NH_2-MIL-125(Ti) structure. Yellow spheres represent the void regions inside the octahedral and tetrahedral cages; green polyhedral = Titanium; red = Oxygen; black = Carbon; blue = Nitrogen. (b) representative SEM of NH_2–MIL–125 (Ti); (c)–(d) Effect of NH_2–MIL–125 (Ti) loading amounts in polysulfone MMM on CO_2 and CH_4 permeability performances. Ref. [219]. (For interpretation of the references to colour in this figure legend, the reader is referred to the Web version of this article.)

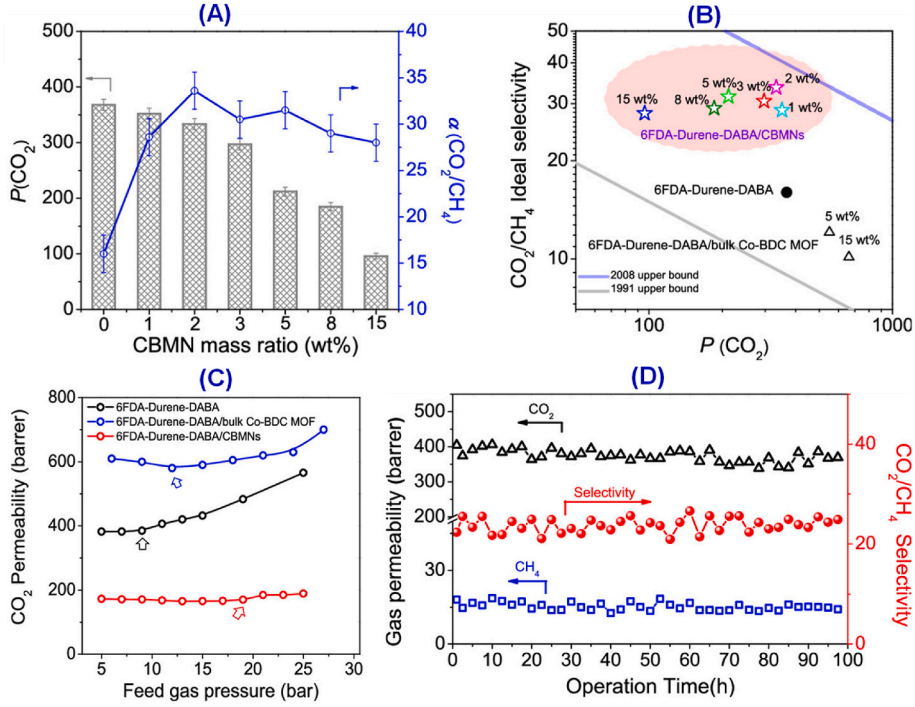

Fig. 12. (a) Effect of MOF Co-benzene dicarboxylate (CBMN) nanofiller loading amount on the performance of MMM composite derived from carboxyl-functionalized polyimide (6FDA-durene-DABA) membrane for CO_2 permeability and CO_2/CH_4 separation selectivity, **(b)** Comparison the performance of CBMN/6FDA-durene-DABA MMM for CO_2/CH_4 selectivity vs CO_2 permeability concerning standardised upper bound 1991 and 2008 data, **(c)** Effect of operating pressure increase on CO_2 permeability performance for 6FDA-durene-DABA membrane and its 6FDA-durene-DABA/CBMN MMM of various MOFs, and **(d)** Long term performance of permeability and selectivity of CO_2 and mixed CO_2/CH_4 over 6FDA-durene-DABA/CBMN MMM with 2 wt % CBMN loading. Ref. [234].

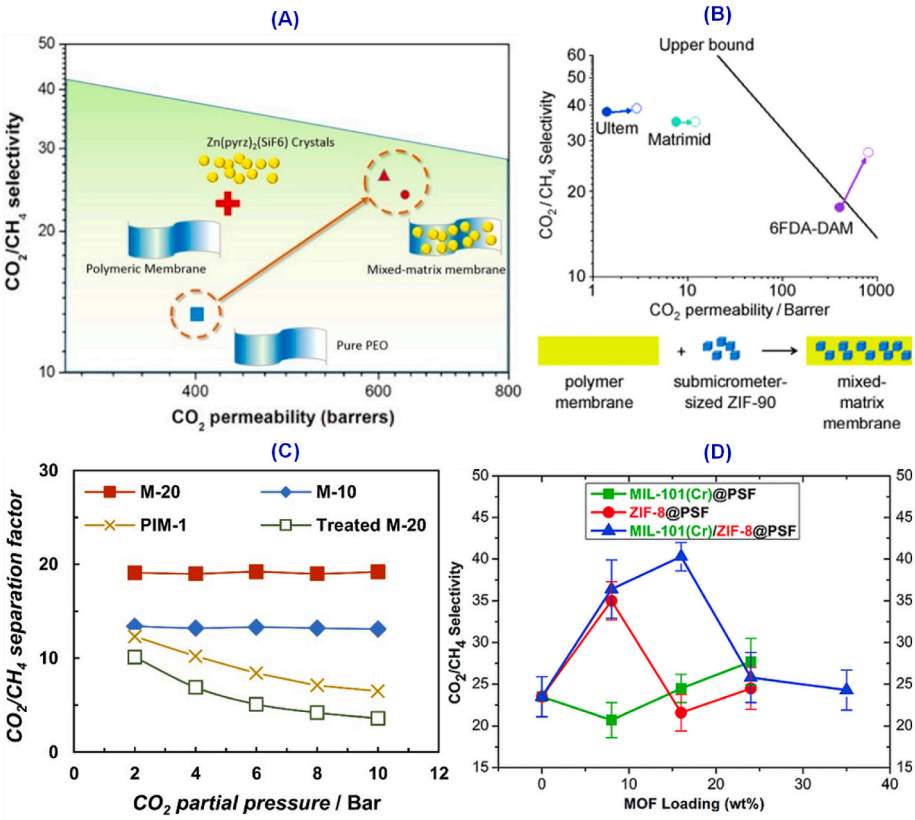

Fig. 13. **(a)** CO_2 permeability and CO_2/CH_4 separation selectivity of $Zn(pyre)_2(SiF_6)$ MOF and its MMM. **(b)** Comparison of sub-micrometer-sized ZIF-90 crystals and its MMM (ZIF-90/6FDA-DAM) CO_2/CH_4 separation selectivity and CO_2 permeability. **(c)** Mixed CO_2/CH_4 gases separation factors for PIM-1 membrane and its MMMs composite with MOF-74 as a function of CO_2 partial pressure (measured with CO_2: CH_4, 1:1 mixture at 25 °C). **(d)** CO_2 permeability and CO_2/CH_4 separation selectivity of MOFs MIL-101(Cr) and ZIF-8 hybridized with polysulfone to construct MMMs composite. Refs. [220,235–237].

CH_4/CO_2 selectivity for ZIF-8/Matrimid MMM with 50 wt% ZIF-8 loading. In another study, the gas transport properties of MMM interfaced with Bio-MOF-1 loading of up to 30 wt% resulted in enhanced CO_2 permeability of 16.57 Barrer and selectivity of 42.6 and 45.6 for CH_4/CO_2 and N_2/CO_2, respectively. This corresponded to an increase of 168% and 58% for CO_2 permeability and selectivity, respectively, compared to pristine polymer membranes [245]. An improved CO_2 separation from the CH_4/CO_2 gas mixture was demonstrated by Zornoza et al. [221] by loading 40 wt% MIL-53 in the MMM composite. Elsewhere, Shahid et al. [246] achieved a two-fold enhancement in both single gas CO_2 permeability to reach 24 Barrer and CH_4/CO_2 selectivity of 66 by incorporating 30 wt% of MIL-53(Al) into Matrimid® polymer to construct an effective MMM composite. MOF-based membranes have superior CO_2 separation capabilities for biogas upgrading. In the biogas cleaning and upgrade, not only CH_4/CO_2 gases are present but also trace contaminants such as H_2S, SO_2, NH_3, siloxanes, and volatile organic compounds, including moisture, which is detrimental to the potential downstream application of biogas-derived CH_4/CO_2. Removing these biogas trace contaminants using MOF-based membranes has also attracted the attention of many researchers worldwide. However, it is still in the infancy stage with limited reported applications. For example, for CO_2 removal, the appropriate selection of the MOF filler and polymer membrane matrix is critical in determining the removal efficiency.

9. Conclusion

This review discussed the current growing developmental updates in the metal-organic framework (MOF) derived sorbent materials for their application in biogas cleaning (i.e., removal of hydrogen sulfide, ammonia, siloxanes, nitrogen, and moisture) and upgrading (i.e., separation of carbon dioxide and methane, CO_2/CH_4). It focused on elaborating how the inherent structure properties of MOFs, such as suitable pore size and volume, high surface area, surface functionalities, and cavity architectures that are characteristic of MOFs, affect their performance in attaining high adsorption removal and separation efficiencies of biogas impurities and targeted CO_2/CH_4, respectively. It further discussed the effect of basic-acidic sites and the coordinated open metal sites in controlling the adsorption of the molecules on their surfaces, including the mechanical aspects related to desorption to achieve the desired high gas separation selectivity. The reviewed data showed a significant impact of the MOF's surface acid/primary sites together with the nature of the metal as critical to achieving high permeability and permeation selective separation of the CO_2/CH_4 gas mixture. Moreover, modifying MOFs to make composites was highlighted as a significant strategy to improve the surface adsorption sites of the MOFs, resulting in enhanced performance in removing biogas impurities and improving CO_2/CH_4 upgrading efficiencies. Finally, adapting MOFs as filler materials for integration in membrane technology to develop advanced mixed-matrix membranes (MMMs) systems demonstrated an effective breakthrough technology development in biogas cleaning and upgrading. The design of MOF-impregnated membranes highlights a potential economic technology that could accelerate the adoption of biogas feedstock in the industrial sector more rapidly to achieve the targets set for a more circular economy. Through the beneficiation of municipal and other waste sources, renewable energy, green chemicals, and other green-derived materials can be produced and thus encompass the circular economy concept. While MOF sorbents and their counterpart integrated membranes have demonstrated potential effectivity in biogas cleaning and upgrading, there are, however, several observed shortcomings that would still require further research and development, such as:

(i) In-depth studies on the developed materials' long-term stability and deactivation performance are needed. Understanding how the materials deactivate is critical in this case. Also, how the deactivation can be reversed at lower energy consumption will prove that MOFs are potential sorbents for industrial applications in biogas cleaning and upgrading.

(ii) Studies on MOF integration in membranes are still emerging, and more baseline performance evaluations coupled with modelling are needed for standardisation, especially for long-term stability performances.

(iii) Most of the reported data for applications and demonstrations of MOFs and MOF-incorporated membranes are applied individually in biogas impurities removal or CO_2/CH_4 upgrading. Few to no studies focus on applying pure MOF materials in membranes which showed lower performance when compared to modified MOF integrated MMMs in the complete removal of biogas impurities and CO_2/CH_4 in a single integrated step. The approach of using modified MOFs integrated with MMMs will provide an economical technology with a huge potential application in the biogas feedstock processing space.

(iv) With the recent emergence of new types of MOFs-based bimetallic or multimetallic composites, the adoption of these new MOF materials could perhaps improve the performances of the neat MOF sorbents, especially in the pre-cleanup stage of gases such as H2S, NH3, etc. prior to CO_2/CH_4 separation.

(v) Finally, the literature is substantially lacking in using raw biogas samples apart from mostly simulated CO_2/CH_4 and trace impurities standards in many studies applying MOFs and their integrated MMMs.

(vi) Modelling has proven to be significantly critical in designing MOFs, which reduces the time and cost of optimising their properties through trial-and-error laboratory work. We propose a similar approach in designing MOFs and their membrane composites with enhanced and durable surface-active sites that could be easily translated into practical industrial applications.

CRediT authorship contribution statement

Zama Duma: Writing – original draft, Formal analysis, Data curation, Conceptualization. **Peter R. Makgwane:** Writing – review & editing, Writing – original draft, Validation, Supervision, Project administration, Formal analysis, Data curation, Conceptualization. **Mike Masukume:** Writing – original draft, Formal analysis, Data curation. **Ashton Swartbooi:** Writing – original draft, Funding acquisition, Formal analysis, Data curation. **Khavharendwe Rambau:** Writing – original draft, Data curation, Conceptualization. **Thembelihle Mehlo:** Writing – original draft, Formal analysis. **Tshidzani Mavhungu:** Writing – review & editing, Formal analysis.

Declaration of competing interest

The authors declare that they have no known competing financial interests or personal relationships that could have appeared to influence the work reported in this paper.

Data availability

The authors do not have permission to share data.

Acknowledgements

The authors are grateful for the financial support of the Council for Scientific and Industrial Research parliamentary grant (CSIR-PG C1G0078).

References

[1] D. Otter, S.-J. Ernst, L. Krätz, H.-J. Bart, Kinetic separation of CO2/CH4 mixtures with Ni-MOF-74 @ Al2O3 core–shell composites, SN Appl. Sci. 2 (2020) 1071, https://doi.org/10.1007/s42452-020-2885-y.

[2] Y. Guo, Y. Yang, M. Bradshaw, C. Wang, M. Blondeel, Globalization and decarbonization: changing strategies of global oil and gas companies, WIREs Climate Change 14 (2023) e849, https://doi.org/10.1002/wcc.849.

[3] Y. Qiu, P. Lamers, V. Daioglou, N. McQueen, H.-S. de Boer, M. Harmsen, J. Wilcox, A. Bardow, S. Suh, Environmental trade-offs of direct air capture technologies in climate change mitigation toward 2100, Nat. Commun. 13 (2022) 3635, https://doi.org/10.1038/s41467-022-31146-1.

[4] P.F. Borowski, Mitigating climate change and the development of green energy versus a return to fossil fuels due to the energy crisis in 2022, Energies 15 (2022), https://doi.org/10.3390/en15249289.

[5] G.S. Seck, E. Hache, J. Sabathier, F. Guedes, G.A. Reigstad, J. Straus, O. Wolfgang, J.A. Ouassou, M. Askeland, I. Hjorth, H.I. Skjelbred, L.E. Andersson, S. Douguet, M. Villavicencio, J. Trüby, J. Brauer, C. Cabot, Hydrogen and the decarbonization of the energy system in europe in 2050: a detailed model-based analysis, Renew. Sustain. Energy Rev. 167 (2022) 112779, https://doi.org/10.1016/j.rser.2022.112779.

[6] M.-K. Kazi, F. Eljack, M.M. El-Halwagi, M. Haouari, Green Hydrogen for Industrial Sector Decarbonization: Costs and Impacts on Hydrogen Economy in qatar, vol. 145, Computers & Chemical Engineering, 2021 107144, https://doi.org/10.1016/j.compchemeng.2020.107144.

[7] B.S. Thapa, B. Neupane, H. Yang, Y.-H. Lee, Green hydrogen potentials from surplus hydro energy in Nepal, Int. J. Hydrogen Energy 46 (2021) 22256–22267, https://doi.org/10.1016/j.ijhydene.2021.04.096.

[8] D. Parra, M. Gillott, G.S. Walker, The role of hydrogen in achieving the decarbonization targets for the UK domestic sector, Int. J. Hydrogen Energy 39 (2014) 4158–4169, https://doi.org/10.1016/j.ijhydene.2014.01.023.

[9] A.G. Olabi, M.A. Abdelkareem, Renewable energy and climate change, Renew. Sustain. Energy Rev. 158 (2022) 112111, https://doi.org/10.1016/j.rser.2022.112111.

[10] H.A. Behabtu, M. Messagie, T. Coosemans, M. Berecibar, K. Anlay Fante, A. A. Kebede, J.V. Mierlo, A review of energy storage technologies' application potentials in renewable energy sources grid integration, Sustainability 12 (2020), https://doi.org/10.3390/su122410511.

[11] M. Balat, H. Balat, Biogas as a renewable energy source—a review, Energy Sources, Part A Recovery, Util. Environ. Eff. 31 (2009) 1280–1293, https://doi.org/10.1080/15567030802089565.

[12] V. Novotny, From biogas-to hydrogen – based integrated urban water, energy and waste solids system - quest towards decarbonization, Int. J. Hydrogen Energy 47 (2022) 10508–10530, https://doi.org/10.1016/j.ijhydene.2022.01.085.

[13] R. Muñoz, L. Meier, I. Diaz, D. Jeison, A review on the state-of-the-art of physical/chemical and biological technologies for biogas upgrading, Rev. Environ. Sci. Biotechnol. 14 (2015) 727–759, https://doi.org/10.1007/s11157-015-9379-1.

[14] N. Yasmin, P. Grundmann, Adoption and diffusion of renewable energy – the case of biogas as alternative fuel for cooking in Pakistan, Renew. Sustain. Energy Rev. 101 (2019) 255–264, https://doi.org/10.1016/j.rser.2018.10.011.

[15] I. Ullah Khan, M. Hafiz Dzarfan Othman, H. Hashim, T. Matsuura, A.F. Ismail, M. Rezaei-DashtArzhandi, I. Wan Azelee, Biogas as a renewable energy fuel – a review of biogas upgrading, utilisation and storage, Energy Convers. Manag. 150 (2017) 277–294, https://doi.org/10.1016/j.enconman.2017.08.035.

[16] V. Ezekoye, D. Ezekoye, A. Ofomatah, A. Agbaogu, Comparative study of calorific values and proximate analysis of biogas from different feedstocks, IOP Conf. Ser. Earth Environ. Sci. 730 (2021) 012018, https://doi.org/10.1088/1755-1315/730/1/012018.

[17] R. Rocher-Rivas, A. González-Sánchez, G. Ulloa-Mercado, R. Muñoz, G. Quijano, Biogas desulfurization and calorific value enhancement in compact H2S/CO2 absorption units coupled to a photobioreactor, J. Environ. Chem. Eng. 10 (2022) 108336, https://doi.org/10.1016/j.jece.2022.108336.

[18] M. Sahin, M. Ilbas, Analysis of the effect of H2O content on combustion behaviours of a biogas fuel, Int. J. Hydrogen Energy 45 (2020) 3651–3659, https://doi.org/10.1016/j.ijhydene.2019.02.042.

[19] H.A. Alabaş, B. Albayrak Çeper, Effect of oxygen enrichment on the combustion characteristic and pollutant emissions of kerosene-biogas mixtures on a mini jet engine combustion chamber, J. Energy Inst. 111 (2023) 101420, https://doi.org/10.1016/j.joei.2023.101420.

[20] M. Alrbai, A.D. Ahmad, S. Al-Dahidi, A.M. Abubaker, L. Al-Ghussain, A. Alahmer, N.K. Akafuah, Performance and sensitivity analysis of raw biogas combustion under homogenous charge compression ignition conditions, Energy 283 (2023) 128486, https://doi.org/10.1016/j.energy.2023.128486.

[21] K. Ciahotný, V. Kyselová, Hydrogen sulfide removal from biogas using carbon impregnated with oxidants, Energy Fuel. 33 (2019) 5316–5321, https://doi.org/10.1021/acs.energyfuels.9b00624.

[22] E. Ryckebosch, M. Drouillon, H. Vervaeren, Techniques for transformation of biogas to biomethane, Biomass Bioenergy 35 (2011) 1633–1645, https://doi.org/10.1016/j.biombioe.2011.02.033.

[23] W. Quan, X. Jiang, X. Wang, C. Song, Hydrogen sulfide removal from biogas on ZIF-derived nitrogen-doped carbons, Catal. Today 371 (2021) 221–230, https://doi.org/10.1016/j.cattod.2020.07.065.

[24] M. Fdz-Polanco, I. Díaz, S.I. Pérez, A.C. Lopes, F. Fdz-Polanco, Hydrogen sulphide removal in the anaerobic digestion of sludge by micro-aerobic processes: pilot plant experience, Water Sci. Technol. 60 (2009) 3045–3050, https://doi.org/10.2166/wst.2009.738.

[25] D. Erdirencelebi, M. Kucukhemek, Control of hydrogen sulphide in full-scale anaerobic digesters using iron (III) chloride: performance, origin and effects, WaterSA 44 (2018), https://doi.org/10.4314/wsa.v44i2.04.
[26] E. Naeiji, A. Noorpoor, H. Ghanavati, Energy, exergy, and economic analysis of cryogenic distillation and chemical scrubbing for biogas upgrading and hydrogen production, Sustainability 14 (2022), https://doi.org/10.3390/su14063686.
[27] E. Tilahun, A. Bayrakdar, E. Sahinkaya, B. Çalli, Performance of polydimethylsiloxane membrane contactor process for selective hydrogen sulfide removal from biogas, Waste Manag. 61 (2017) 250–257, https://doi.org/10.1016/j.wasman.2017.01.011.
[28] S. Sahota, V.K. Vijay, P.M.V. Subbarao, R. Chandra, P. Ghosh, G. Shah, R. Kapoor, V. Vijay, V. Koutu, I.S. Thakur, Characterization of leaf waste based biochar for cost effective hydrogen sulphide removal from biogas, Bioresour. Technol. 250 (2018) 635–641, https://doi.org/10.1016/j.biortech.2017.11.093.
[29] M.S. Horikawa, F. Rossi, M.L. Gimenes, C.M.M. Costa, M.G.C. da Silva, Chemical absorption of H2S for biogas purification, Braz. J. Chem. Eng. 21 (2004).
[30] E. Mulu, M.M. M'Arimi, R.C. Ramkat, A review of recent developments in application of low cost natural materials in purification and upgrade of biogas, Renew. Sustain. Energy Rev. 145 (2021) 111081, https://doi.org/10.1016/j.rser.2021.111081.
[31] T. Tuerhong, Z. Kuerban, Preparation and characterization of cattle manure-based activated carbon for hydrogen sulfide removal at room temperature, J. Environ. Chem. Eng. 10 (2022) 107177, https://doi.org/10.1016/j.jece.2022.107177.
[32] H. Sawalha, M. Maghalseh, J. Qutaina, K. Junaidi, E.R. Rene, Removal of hydrogen sulfide from biogas using activated carbon synthesized from different locally available biomass wastes - a case study from Palestine, Bioengineered 11 (2020) 607–618, https://doi.org/10.1080/21655979.2020.1768736.
[33] H. Daglar, S. Keskin, Recent advances, opportunities, and challenges in high-throughput computational screening of MOFs for gas separations, Coord. Chem. Rev. 422 (2020) 213470, https://doi.org/10.1016/j.ccr.2020.213470.
[34] R. Chen, M. Chai, J. Hou, Metal-organic framework-based mixed matrix membranes for gas separation: recent advances and opportunities, Carbon Capture Science & Technology 8 (2023) 100130, https://doi.org/10.1016/j.ccst.2023.100130.
[35] R. Chen, M. Chai, J. Hou, Metal-organic framework-based mixed matrix membranes for gas separation: recent advances and opportunities, Carbon Capture Science & Technology 8 (2023) 100130, https://doi.org/10.1016/j.ccst.2023.100130.
[36] Q. Qian, P.A. Asinger, M.J. Lee, G. Han, K. Mizrahi Rodriguez, S. Lin, F. M. Benedetti, A.X. Wu, W.S. Chi, Z.P. Smith, MOF-based membranes for gas separations, Chem. Rev. 120 (2020) 8161–8266, https://doi.org/10.1021/acs.chemrev.0c00119.
[37] G. Lu, F. Chu, X. Huang, Y. Li, K. Liang, G. Wang, Recent advances in Metal-Organic Frameworks-based materials for photocatalytic selective oxidation, Coord. Chem. Rev. 450 (2022) 214240, https://doi.org/10.1016/j.ccr.2021.214240.
[38] A. Ahmad, S. Khan, S. Tariq, R. Luque, F. Verpoort, Self-sacrifice MOFs for heterogeneous catalysis: synthesis mechanisms and future perspectives, Mater. Today 55 (2022) 137–169, https://doi.org/10.1016/j.mattod.2022.04.002.
[39] T.A. Goetjen, J. Liu, Y. Wu, J. Sui, X. Zhang, J.T. Hupp, O.K. Farha, Metal–organic framework (MOF) materials as polymerization catalysts: a review and recent advances, Chem. Commun. 56 (2020) 10409–10418, https://doi.org/10.1039/D0CC03790G.
[40] H. Konnerth, B.M. Matsagar, S.S. Chen, M.H.G. Prechtl, F.-K. Shieh, K.C.-W. Wu, Metal-organic framework (MOF)-derived catalysts for fine chemical production, Coord. Chem. Rev. 416 (2020) 213319, https://doi.org/10.1016/j.ccr.2020.213319.
[41] B. Chen, Z. Yang, Q. Jia, R.J. Ball, Y. Zhu, Y. Xia, Emerging applications of metal-organic frameworks and derivatives in solar cells: recent advances and challenges, Mater. Sci. Eng. R Rep. 152 (2023) 100714, https://doi.org/10.1016/j.mser.2022.100714.
[42] Y. Shi, A.-F. Yang, C.-S. Cao, B. Zhao, Applications of MOFs: recent advances in photocatalytic hydrogen production from water, Coord. Chem. Rev. 390 (2019) 50–75, https://doi.org/10.1016/j.ccr.2019.03.012.
[43] D.Y. Heo, H.H. Do, S.H. Ahn, S.Y. Kim, Metal-organic framework materials for perovskite solar cells, Polymers 12 (2020), https://doi.org/10.3390/polym12092061.
[44] L. Lu, B. Wu, W. Shi, P. Cheng, Metal–organic framework-derived heterojunctions as nanocatalysts for photocatalytic hydrogen production, Inorg. Chem. Front. 6 (2019) 3456–3467, https://doi.org/10.1039/C9QI00964G.
[45] Y. Peng, J. Xu, J. Xu, J. Ma, Y. Bai, S. Cao, S. Zhang, H. Pang, Metal-organic framework (MOF) composites as promising materials for energy storage applications, Adv. Colloid Interface Sci. 307 (2022) 102732, https://doi.org/10.1016/j.cis.2022.102732.
[46] S.P. Shet, S. Shanmuga Priya, K. Sudhakar, M. Tahir, A review on current trends in potential use of metal-organic framework for hydrogen storage, Int. J. Hydrogen Energy 46 (2021) 11782–11803, https://doi.org/10.1016/j.ijhydene.2021.01.020.
[47] V. Kudiiarov, J. Lyu, O. Semyonov, A. Lider, S. Chaemchuen, F. Verpoort, Prospects of hybrid materials composed of MOFs and hydride-forming metal nanoparticles for light-duty vehicle hydrogen storage, Appl. Mater. Today 25 (2021) 101208, https://doi.org/10.1016/j.apmt.2021.101208.
[48] A. Khan, M.A. Qyyum, H. Saulat, R. Ahmad, X. Peng, M. Lee, Metal–organic frameworks for biogas upgrading: recent advancements, challenges, and future recommendations, Appl. Mater. Today 22 (2021) 100925, https://doi.org/10.1016/j.apmt.2020.100925.
[49] P. Tanvidkar, S. Appari, B.V.R. Kuncharam, A review of techniques to improve performance of metal organic framework (MOF) based mixed matrix membranes for CO2/CH4 separation, Rev. Environ. Sci. Biotechnol. 21 (2022) 539–569, https://doi.org/10.1007/s11157-022-09612-5.
[50] M. Yusuf, R. Kumar, M. Ali Khan, M.J. Ahmed, M. Otero, S. Muthu Prabhu, M. Son, J.-H. Hwang, W. Hyoung Lee, B.-H. Jeon, Metal-organic framework-based composites for biogas and natural gas uptake: an overview of adsorption and storage mechanisms of gaseous fuels, Chem. Eng. J. 478 (2023) 147302, https://doi.org/10.1016/j.cej.2023.147302.
[51] R. Sahoo, S. Mondal, D. Mukherjee, M.C. Das, Metal–organic frameworks for CO2 separation from flue and biogas mixtures, Adv. Funct. Mater. 32 (2022) 2207197, https://doi.org/10.1002/adfm.202207197.
[52] R. Sahoo, S. Mondal, D. Mukherjee, M.C. Das, Metal–organic frameworks for CO2 separation from flue and biogas mixtures, Adv. Funct. Mater. 32 (2022) 2207197, https://doi.org/10.1002/adfm.202207197.
[53] J.H. Choe, H. Kim, C.S. Hong, MOF-74 type variants for CO2 capture, Mater. Chem. Front. 5 (2021) 5172–5185, https://doi.org/10.1039/D1QM00205H.
[54] M. Younas, M. Rezakazemi, M. Daud, M.B. Wazir, S. Ahmad, N. UllahInamuddin, S. Ramakrishna, Recent progress and remaining challenges in post-combustion CO2 capture using metal-organic frameworks (MOFs), Prog. Energy Combust. Sci. 80 (2020) 100849, https://doi.org/10.1016/j.pecs.2020.100849.
[55] M. Usman, N. Iqbal, T. Noor, N. Zaman, A. Asghar, M.M. Abdelnaby, A. Galadima, A. Helal, Advanced strategies in metal-organic frameworks for CO2 capture and separation, Chem. Rec. 22 (2022) e202100230, https://doi.org/10.1002/tcr.202100230.
[56] A. Khan, M.A. Qyyum, H. Saulat, R. Ahmad, X. Peng, M. Lee, Metal–organic frameworks for biogas upgrading: recent advancements, challenges, and future recommendations, Appl. Mater. Today 22 (2021) 100925, https://doi.org/10.1016/j.apmt.2020.100925.
[57] J.E. Castellanos-Sánchez, F.A. Aguilar-Aguilar, R. Hernández-Altamirano, J.A. Venegas Venegas, D. Raj Aryal, Biogas purification processes: review and prospects, Biofuels (n.d.) 1–13 https://doi.org/10.1080/17597269.2023.2223801..
[58] R. Kapoor, P. Ghosh, B. Tyagi, V.K. Vijay, V. Vijay, I.S. Thakur, H. Kamyab, D. D. Nguyen, A. Kumar, Advances in biogas valorization and utilization systems: a comprehensive review, J. Clean. Prod. 273 (2020) 123052, https://doi.org/10.1016/j.jclepro.2020.123052.
[59] A. Golmakani, S. Ali Nabavi, B. Wadi, V. Manovic, Advances, challenges, and perspectives of biogas cleaning, upgrading, and utilisation, Fuel 317 (2022) 123085, https://doi.org/10.1016/j.fuel.2021.123085.
[60] O.W. Awe, Y. Zhao, A. Nzihou, D.P. Minh, N. Lyczko, A review of biogas utilisation, purification and upgrading technologies, Waste and Biomass Valorization 8 (2017) 267–283, https://doi.org/10.1007/s12649-016-9826-4.
[61] M.R. Atelge, H. Senol, M. Djaafri, T.A. Hansu, D. Krisa, A. Atabani, C. Eskicioglu, H. Muratçobanoğlu, S. Unalan, S. Kalloum, N. Azbar, H.D. Kıvrak, A critical overview of the state-of-the-art methods for biogas purification and utilization processes, Sustainability 13 (2021), https://doi.org/10.3390/su132011515.
[62] X.Y. Chen, H. Vinh-Thang, A.A. Ramirez, D. Rodrigue, S. Kaliaguine, Membrane gas separation technologies for biogas upgrading, RSC Adv. 5 (2015) 24399–24448, https://doi.org/10.1039/C5RA00666J.
[63] F.M. Baena-Moreno, M. Gonzalez-Castaño, H. Arellano-García, T.R. Reina, Exploring profitability of bioeconomy paths: dimethyl ether from biogas as case study, Energy 225 (2021) 120230, https://doi.org/10.1016/j.energy.2021.120230.
[64] P. Rosha, A.K. Rosha, H. Ibrahim, S. Kumar, Recent advances in biogas upgrading to value added products: a review, Int. J. Hydrogen Energy 46 (2021) 21318–21337, https://doi.org/10.1016/j.ijhydene.2021.03.246.
[65] Z.G. Duma, X. Dyosiba, J. Moma, H.W. Langmi, B. Louis, K. Parkhomenko, N. M. Musyoka, Thermocatalytic hydrogenation of CO2 to methanol using Cu-ZnO bimetallic catalysts supported on metal–organic frameworks, Catalysts 12 (2022), https://doi.org/10.3390/catal12040401.
[66] A. Golmakani, S. Ali Nabavi, B. Wadi, V. Manovic, Advances, challenges, and perspectives of biogas cleaning, upgrading, and utilisation, Fuel 317 (2022) 123085, https://doi.org/10.1016/j.fuel.2021.123085.
[67] P.G. Kougias, I. Angelidaki, Biogas and its opportunities—a review, Front. Environ. Sci. Eng. 12 (2018) 14, https://doi.org/10.1007/s11783-018-1037-8.
[68] H. Wasajja, R.E.F. Lindeboom, J.B. van Lier, P.V. Aravind, Techno-economic review of biogas cleaning technologies for small scale off-grid solid oxide fuel cell applications, Fuel Process. Technol. 197 (2020) 106215, https://doi.org/10.1016/j.fuproc.2019.106215.
[69] D. Bertasini, F. Battista, F. Rizzioli, N. Frison, D. Bolzonella, Decarbonization of the European natural gas grid using hydrogen and methane biologically produced from organic waste: a critical overview, Renew. Energy 206 (2023) 386–396, https://doi.org/10.1016/j.renene.2023.02.029.
[70] C.-C. Cormos, A.-M. Cormos, L. Petrescu, S. Dragan, Techno-economic assessment of decarbonized biogas catalytic reforming for flexible hydrogen and power production, Appl. Therm. Eng. 207 (2022) 118218, https://doi.org/10.1016/j.applthermaleng.2022.118218.
[71] M. Pudukudy, Z. Yaakob, K. Mhd Syahri, Q. Jia, S. Shan, Production of hydrogen-rich syngas and multiwalled carbon nanotubes by biogas decomposition over zirconia supported iron catalysts, J. Ind. Eng. Chem. 84 (2020) 150–166, https://doi.org/10.1016/j.jiec.2019.12.030.
[72] T. Kludpantanapan, P. Nantapong, R. Rattanaamonkulchai, A. Srifa, W. Koo-Amornpattana, W. Chaiwat, C. Sakdaronnarong, T. Charinpanitkul,

S. Assabumrungrat, S. Wongsakulphasatch, M. Sudoh, R. Watanabe, C. Fukuhara, S. Ratchahat, Simultaneous production of hydrogen and carbon nanotubes from biogas: on the effect of Ce addition to CoMo/MgO catalyst, Int. J. Hydrogen Energy 46 (2021) 38175–38190, https://doi.org/10.1016/j.ijhydene.2021.09.068.
[73] Z.G. Duma, A. Swartbooi, N.M. Musyoka, Thermocatalytic decomposition of methane to low-carbon hydrogen using LaNi1-xCuxO3 perovskite catalysts, Appl. Catal. Gen. 677 (2024) 119703, https://doi.org/10.1016/j.apcata.2024.119703.
[74] J. Annamalai, P. Murugan, D. Ganapathy, D. Nallaswamy, R. Atchudan, S. Arya, A. Khosla, S. Barathi, A.K. Sundramoorthy, Synthesis of various dimensional metal organic frameworks (MOFs) and their hybrid composites for emerging applications – a review, Chemosphere 298 (2022) 134184, https://doi.org/10.1016/j.chemosphere.2022.134184.
[75] S. Qiu, G. Zhu, Molecular engineering for synthesizing novel structures of metal–organic frameworks with multifunctional properties, Coord. Chem. Rev. 253 (2009) 2891–2911, https://doi.org/10.1016/j.ccr.2009.07.020.
[76] N. Al Amery, H.R. Abid, S. Al-Saadi, S. Wang, S. Liu, Facile directions for synthesis, modification and activation of MOFs, Mater. Today Chem. 17 (2020) 100343, https://doi.org/10.1016/j.mtchem.2020.100343.
[77] P. Bhakat, A. Nigam, S. Jagtap, Green synthesis of MOF nanostructures: environmental benefits and applications, Nanotechnology for Environmental Engineering 8 (2023) 815–827, https://doi.org/10.1007/s41204-023-00325-w.
[78] L. Ge, T. Ge, R. Wang, Facile synthesis of Al-based MOF and its applications in desiccant coated heat exchangers, Renew. Sustain. Energy Rev. 157 (2022) 112015, https://doi.org/10.1016/j.rser.2021.112015.
[79] T. Wang, H. Zhu, Q. Zeng, D. Liu, Strategies for overcoming defects of HKUST-1 and its relevant applications, Adv. Mater. Interfac. 6 (2019) 1900423, https://doi.org/10.1002/admi.201900423.
[80] K.O. Otun, S.O. Amusat, I.T. Bello, J. Abdulsalam, A.T. Ajiboye, A.A. Adeleke, S. O. Azeez, Recent advances in the synthesis of various analogues of MOF-based nanomaterials: a mini-review, Inorg. Chim. Acta. 536 (2022) 120890, https://doi.org/10.1016/j.ica.2022.120890.
[81] T. Gao, H.-J. Tang, S.-Y. Zhang, J.-W. Cao, Y.-N. Wu, J. Chen, Y. Wang, K.-J. Chen, Mechanochemical synthesis of three-component metal-organic frameworks for large scale production, J. Solid State Chem. 303 (2021) 122547, https://doi.org/10.1016/j.jssc.2021.122547.
[82] J. Beamish-Cook, K. Shankland, C.A. Murray, P. Vaqueiro, Insights into the mechanochemical synthesis of MOF-74, Cryst. Growth Des. 21 (2021) 3047–3055, https://doi.org/10.1021/acs.cgd.1c00213.
[83] B. Szczęśniak, S. Borysiuk, J. Choma, M. Jaroniec, Mechanochemical synthesis of highly porous materials, Mater. Horiz. 7 (2020) 1457–1473, https://doi.org/10.1039/D0MH00081G.
[84] S. Głowniak, B. Szczęśniak, J. Choma, M. Jaroniec, Mechanochemistry: toward green synthesis of metal–organic frameworks, Mater. Today 46 (2021) 109–124, https://doi.org/10.1016/j.mattod.2021.01.008.
[85] C. Vaitsis, G. Sourkouni, C. Argirusis, Chapter 11 - sonochemical synthesis of MOFs, in: M. Mozafari (Ed.), Metal-Organic Frameworks for Biomedical Applications, Woodhead Publishing, 2020, pp. 223–244, https://doi.org/10.1016/B978-0-12-816984-1.00013-5.
[86] B. Yang, J. Huang, J. Tong, H. Peng, Y. Xiang, M. Ruan, Z. Chen, Z. Yang, W. Xiong, Microwave synthesis of Fe–Cu diatomic active center MOF: synergistic cyclic catalysis of persulfate for degrading norfloxacin, Environ. Sci.: Nano 10 (2023) 2778–2789, https://doi.org/10.1039/D3EN00340J.
[87] K. Yu, Y.-R. Lee, J.Y. Seo, K.-Y. Baek, Y.-M. Chung, W.-S. Ahn, Sonochemical synthesis of Zr-based porphyrinic MOF-525 and MOF-545: enhancement in catalytic and adsorption properties, Microporous Mesoporous Mater. 316 (2021) 110985, https://doi.org/10.1016/j.micromeso.2021.110985.
[88] L. Yang, H. Lu, Microwave-assisted ionothermal synthesis and characterization of zeolitic imidazolate framework-8, Chin. J. Chem. 30 (2012) 1040–1044, https://doi.org/10.1002/cjoc.201100595.
[89] W.J. Phang, W.R. Lee, K. Yoo, D.W. Ryu, B. Kim, C.S. Hong, pH-dependent proton conducting behavior in a metal–organic framework material, Angew. Chem. Int. Ed. 53 (2014) 8383–8387, https://doi.org/10.1002/anie.201404164.
[90] R. Sabouni, H. Kazemian, S. Rohani, Microwave synthesis of the CPM-5 metal organic framework, Chem. Eng. Technol. 35 (2012) 1085–1092, https://doi.org/10.1002/ceat.201100626.
[91] J. Ru, X. Wang, F. Wang, X. Cui, X. Du, X. Lu, UiO series of metal-organic frameworks composites as advanced sorbents for the removal of heavy metal ions: synthesis, applications and adsorption mechanism, Ecotoxicol. Environ. Saf. 208 (2021) 111577, https://doi.org/10.1016/j.ecoenv.2020.111577.
[92] F. Ahmadijokani, H. Molavi, M. Rezakazemi, S. Tajahmadi, A. Bahi, F. Ko, T. M. Aminabhavi, J.-R. Li, M. Arjmand, UiO-66 metal–organic frameworks in water treatment: a critical review, Prog. Mater. Sci. 125 (2022) 100904, https://doi.org/10.1016/j.pmatsci.2021.100904.
[93] M.Y. Zorainy, M. Gar Alalm, S. Kaliaguine, D.C. Boffito, Revisiting the MIL-101 metal–organic framework: design, synthesis, modifications, advances, and recent applications, J. Mater. Chem. A 9 (2021) 22159–22217, https://doi.org/10.1039/D1TA06238G.
[94] H. Wang, Q. He, S. Liang, Y. Li, X. Zhao, L. Mao, F. Zhan, L. Chen, Advances and perspectives of ZIFs-based materials for electrochemical energy storage: design of synthesis and crystal structure, evolution of mechanisms and electrochemical performance, Energy Storage Mater. 43 (2021) 531–578, https://doi.org/10.1016/j.ensm.2021.09.023.
[95] B. Chen, Z. Yang, Y. Zhu, Y. Xia, Zeolitic imidazolate framework materials: recent progress in synthesis and applications, J. Mater. Chem. A 2 (2014) 16811–16831, https://doi.org/10.1039/C4TA02984D.
[96] T. Wang, H. Zhu, Q. Zeng, D. Liu, Strategies for overcoming defects of HKUST-1 and its relevant applications, Adv. Mater. Interfac. 6 (2019) 1900423, https://doi.org/10.1002/admi.201900423.
[97] G. Cai, P. Yan, L. Zhang, H.-C. Zhou, H.-L. Jiang, Metal–organic framework-based hierarchically porous materials: synthesis and applications, Chem. Rev. 121 (2021) 12278–12326, https://doi.org/10.1021/acs.chemrev.1c00243.
[98] X. Cai, Z. Xie, D. Li, M. Kassymova, S.-Q. Zang, H.-L. Jiang, Nano-sized metal-organic frameworks: synthesis and applications, Coord. Chem. Rev. 417 (2020) 213366, https://doi.org/10.1016/j.ccr.2020.213366.
[99] S. Kumar, S. Jain, M. Nehra, N. Dilbaghi, G. Marrazza, K.-H. Kim, Green synthesis of metal–organic frameworks: a state-of-the-art review of potential environmental and medical applications, Coord. Chem. Rev. 420 (2020) 213407, https://doi.org/10.1016/j.ccr.2020.213407.
[100] M. Duan, L. Jiang, G. Zeng, D. Wang, W. Tang, J. Liang, H. Wang, D. He, Z. Liu, L. Tang, Bimetallic nanoparticles/metal-organic frameworks: synthesis, applications and challenges, Appl. Mater. Today 19 (2020) 100564, https://doi.org/10.1016/j.apmt.2020.100564.
[101] F. Deng, X.-B. Luo, L. Ding, S.-L. Luo, 5 - application of nanomaterials and nanotechnology in the reutilization of metal ion from wastewater, in: X. Luo, F. Deng (Eds.), Nanomaterials for the Removal of Pollutants and Resource Reutilization, Elsevier, 2019, pp. 149–178, https://doi.org/10.1016/B978-0-12-814837-2.00005-6.
[102] O.D. Agboola, N.U. Benson, Physisorption and chemisorption mechanisms influencing micro (nano) plastics-organic chemical contaminants interactions: a review, Front. Environ. Sci. 9 (2021). https://www.frontiersin.org/articles/10.3389/fenvs.2021.678574.
[103] J.L. Obeso, D.R. Amaro, C.V. Flores, A. Gutiérrez-Alejandre, R.A. Peralta, C. Leyva, I.A. Ibarra, Chemical transformations of highly toxic H2S to promising clean energy in MOFs, Coord. Chem. Rev. 485 (2023) 215135, https://doi.org/10.1016/j.ccr.2023.215135.
[104] K. Ciahotný, V. Kyselová, Hydrogen sulfide removal from biogas using carbon impregnated with oxidants, Energy Fuel. 33 (2019) 5316–5321, https://doi.org/10.1021/acs.energyfuels.9b00624.
[105] P. Cherosky, Y. Li, Hydrogen sulfide removal from biogas by bio-based iron sponge, Biosyst. Eng. 114 (2013) 55–59, https://doi.org/10.1016/j.biosystemseng.2012.10.010.
[106] A. Chidambaram, D.H. Le, J.A.R. Navarro, K.C. Stylianou, Robust metal-organic frameworks for dry and wet biogas upgrading, Appl. Mater. Today 22 (2021) 100933, https://doi.org/10.1016/j.apmt.2020.100933.
[107] S.A. Vali, J. Moral-Vico, X. Font, A. Sánchez, Adsorptive removal of siloxanes from biogas: recent advances in catalyst reusability and water content effect, Biomass Conversion and Biorefinery (2023), https://doi.org/10.1007/s13399-023-04478-1.
[108] K.M.C. Santos, T.R. Menezes, M.R. Oliveira, T.S.L. Silva, K.S. Santos, V.A. Barros, D.C. Melo, A.L. Ramos, C.C. Santana, E. Franceschi, C. Dariva, S.M. Egues, G. R. Borges, J.F. De Conto, Natural gas dehydration by adsorption using MOFs and silicas: a review, Separ. Purif. Technol. 276 (2021) 119409, https://doi.org/10.1016/j.seppur.2021.119409.
[109] L. Jiang, J. Yong, R. Xie, P. Xie, X. Zhang, Z. Chen, Z. Bao, Screening, preparation, and prototyping of metal–organic frameworks for adsorptive carbon capture under humid conditions, SusMat 3 (2023) 609–638, https://doi.org/10.1002/sus2.154.
[110] B. Zhang, Z. Zhu, X. Wang, X. Liu, F. Kapteijn, Water adsorption in MOFs: structures and applications, Advanced Functional Materials n/a (2023) 2304788, https://doi.org/10.1002/adfm.202304788.
[111] D. Andirova, Y. Lei, X. Zhao, S. Choi, Functionalization of metal–organic frameworks for enhanced stability under humid carbon dioxide capture conditions, ChemSusChem 8 (2015) 3405–3409, https://doi.org/10.1002/cssc.201500580.
[112] N.T.T. Nguyen, H. Furukawa, F. Gándara, H.T. Nguyen, K.E. Cordova, O.M. Yaghi, Selective capture of carbon dioxide under humid conditions by hydrophobic chabazite-type zeolitic imidazolate frameworks, Angew. Chem. Int. Ed. 53 (2014) 10645–10648, https://doi.org/10.1002/anie.201403980.
[113] S. Chaemchuen, N.A. Kabir, K. Zhou, F. Verpoort, Metal–organic frameworks for upgrading biogas via CO2 adsorption to biogas green energy, Chem. Soc. Rev. 42 (2013) 9304–9332, https://doi.org/10.1039/C3CS60244C.
[114] Y. Yang, M. Faheem, L. Wang, Q. Meng, H. Sha, N. Yang, Y. Yuan, G. Zhu, Surface pore engineering of covalent organic frameworks for ammonia capture through synergistic multivariate and open metal site approaches, ACS Cent. Sci. 4 (2018) 748–754, https://doi.org/10.1021/acscentsci.8b00232.
[115] J.F. Van Humbeck, T.M. McDonald, X. Jing, B.M. Wiers, G. Zhu, J.R. Long, Ammonia capture in porous organic polymers densely functionalized with brønsted acid groups, J. Am. Chem. Soc. 136 (2014) 2432–2440, https://doi.org/10.1021/ja4105478.
[116] D.K. Yoo, B.N. Bhadra, S.H. Jhung, Adsorptive removal of hazardous organics from water and fuel with functionalized metal-organic frameworks: contribution of functional groups, J. Hazard Mater. 403 (2021) 123655, https://doi.org/10.1016/j.jhazmat.2020.123655.
[117] A. Qajar, M. Peer, M.R. Andalibi, R. Rajagopalan, H.C. Foley, Enhanced ammonia adsorption on functionalized nanoporous carbons, Microporous Mesoporous Mater. 218 (2015) 15–23, https://doi.org/10.1016/j.micromeso.2015.06.030.
[118] D. Saha, S. Deng, Ammonia adsorption and its effects on framework stability of MOF-5 and MOF-177, J. Colloid Interface Sci. 348 (2010) 615–620, https://doi.org/10.1016/j.jcis.2010.04.078.
[119] A.J. Rieth, Y. Tulchinsky, M. Dincă, High and reversible ammonia uptake in mesoporous azolate metal–organic frameworks with open Mn, Co, and Ni sites,

J. Am. Chem. Soc. 138 (2016) 9401–9404, https://doi.org/10.1021/jacs.6b05723.
[120] H.G.W. Godfrey, I. da Silva, L. Briggs, J.H. Carter, C.G. Morris, M. Savage, T. L. Easun, P. Manuel, C.A. Murray, C.C. Tang, M.D. Frogley, G. Cinque, S. Yang, M. Schröder, Ammonia storage by reversible host–guest site exchange in a robust metal–organic framework, Angew. Chem. Int. Ed. 57 (2018) 14778–14781, https://doi.org/10.1002/anie.201808316.
[121] H. Jasuja, G.W. Peterson, J.B. Decoste, M.A. Browe, K.S. Walton, Evaluation of MOFs for air purification and air quality control applications: ammonia removal from air, Chem. Eng. Sci. 124 (2015) 118–124, https://doi.org/10.1016/j.ces.2014.08.050.
[122] S. Glomb, D. Woschko, G. Makhloufi, C. Janiak, Metal–organic frameworks with internal urea-functionalized dicarboxylate linkers for SO2 and NH3 adsorption, ACS Appl. Mater. Interfaces 9 (2017) 37419–37434, https://doi.org/10.1021/acsami.7b10884.
[123] S. Moribe, Z. Chen, S. Alayoglu, Z.H. Syed, T. Islamoglu, O.K. Farha, Ammonia capture within isoreticular metal–organic frameworks with rod secondary building units, ACS Materials Lett 1 (2019) 476–480, https://doi.org/10.1021/acsmaterialslett.9b00307.
[124] L. Guo, J. Hurd, M. He, W. Lu, J. Li, D. Crawshaw, M. Fan, S. Sapchenko, Y. Chen, X. Zeng, M. Kippax-Jones, W. Huang, Z. Zhu, P. Manuel, M.D. Frogley, D. Lee, M. Schröder, S. Yang, Efficient capture and storage of ammonia in robust aluminium-based metal-organic frameworks, Commun. Chem. 6 (2023) 55, https://doi.org/10.1038/s42004-023-00850-4.
[125] A. Takahashi, H. Tanaka, D. Parajuli, T. Nakamura, K. Minami, Y. Sugiyama, Y. Hakuta, S. Ohkoshi, T. Kawamoto, Historical pigment exhibiting ammonia gas capture beyond standard adsorbents with adsorption sites of two kinds, J. Am. Chem. Soc. 138 (2016) 6376–6379, https://doi.org/10.1021/jacs.6b02721.
[126] G. Piechota, Siloxanes in biogas: approaches of sampling procedure and GC-MS method determination, Molecules 26 (2021), https://doi.org/10.3390/molecules26071953.
[127] J. Álvarez-Flórez, E. Egusquiza, Analysis of damage caused by siloxanes in stationary reciprocating internal combustion engines operating with landfill gas, Eng. Fail. Anal. 50 (2015) 29–38, https://doi.org/10.1016/j.engfailanal.2015.01.010.
[128] C.M.A. Eichler, Y. Wu, S.S. Cox, S. Klaus, G.D. Boardman, Evaluation of sampling techniques for gas-phase siloxanes in biogas, Biomass Bioenergy 108 (2018) 1–6, https://doi.org/10.1016/j.biombioe.2017.10.049.
[129] Y. Mito-oka, S. Horike, Y. Nishitani, T. Masumori, M. Inukai, Y. Hijikata, S. Kitagawa, Siloxane D4 capture by hydrophobic microporous materials, J. Mater. Chem. A 1 (2013) 7885–7888, https://doi.org/10.1039/C3TA11217A.
[130] N. Gargiulo, A. Peluso, P. Aprea, O. Marino, R. Cioffi, E. Jannelli, S. Cimino, L. Lisi, D. Caputo, Chromium-based MIL-101 metal organic framework as a fully regenerable D4 adsorbent for biogas purification, Renew. Energy 138 (2019) 230–235, https://doi.org/10.1016/j.renene.2019.01.096.
[131] E. Gulcay-Ozcan, P. Iacomi, Y. Ko, J.-S. Chang, G. Rioland, S. Devautour-Vinot, G. Maurin, Breaking the upper bound of siloxane uptake: metal–organic frameworks as an adsorbent platform, J. Mater. Chem. A 9 (2021) 12711–12720, https://doi.org/10.1039/D1TA02275J.
[132] J. Guo, Y. Luo, A.C. Lua, R. Chi, Y. Chen, X. Bao, S. Xiang, Adsorption of hydrogen sulphide (H2S) by activated carbons derived from oil-palm shell, Carbon 45 (2007) 330–336, https://doi.org/10.1016/j.carbon.2006.09.016.
[133] T. Yu, Z. Chen, Z. Liu, J. Xu, Y. Wang, Review of hydrogen sulfide removal from various industrial gases by zeolites, Separations 9 (2022), https://doi.org/10.3390/separations9090229.
[134] D.M. Cristiano, R. de A. Mohedano, W.C. Nadaleti, A.B. de Castilhos Junior, V. A. Lourenço, D.F.H. Gonçalves, P.B. Filho, H2S adsorption on nanostructured iron oxide at room temperature for biogas purification: application of renewable energy, Renew. Energy 154 (2020) 151–160, https://doi.org/10.1016/j.renene.2020.02.054.
[135] L. Hamon, C. Serre, T. Devic, T. Loiseau, F. Millange, G. Férey, G.D. Weireld, Comparative study of hydrogen sulfide adsorption in the MIL-53(Al, Cr, Fe), MIL-47(V), MIL-100(Cr), and MIL-101(Cr) Metal−Organic frameworks at room temperature, J. Am. Chem. Soc. 131 (2009) 8775–8777, https://doi.org/10.1021/ja901587t.
[136] J. Liu, Y. Wei, P. Li, Y. Zhao, R. Zou, Selective H2S/CO2 separation by metal–organic frameworks based on chemical-physical adsorption, J. Phys. Chem. C 121 (2017) 13249–13255, https://doi.org/10.1021/acs.jpcc.7b04465.
[137] N.K. Gupta, S. Kim, J. Bae, K.S. Kim, Chemisorption of hydrogen sulfide over copper-based metal–organic frameworks: methanol and UV-assisted regeneration, RSC Adv. 11 (2021) 4890–4900, https://doi.org/10.1039/D0RA09017D.
[138] I. Ahmed, S.H. Jhung, Composites of metal–organic frameworks: preparation and application in adsorption, Mater. Today 17 (2014) 136–146, https://doi.org/10.1016/j.mattod.2014.03.002.
[139] N. Bhoria, G. Basina, J. Pokhrel, K.S. Kumar Reddy, S. Anastasiou, V. V. Balasubramanian, Y.F. AlWahedi, G.N. Karanikolos, Functionalization effects on HKUST-1 and HKUST-1/graphene oxide hybrid adsorbents for hydrogen sulfide removal, J. Hazard Mater. 394 (2020) 122565, https://doi.org/10.1016/j.jhazmat.2020.122565.
[140] C. Petit, B. Mendoza, T.J. Bandosz, Hydrogen sulfide adsorption on MOFs and MOF/graphite oxide composites, ChemPhysChem 11 (2010) 3678–3684, https://doi.org/10.1002/cphc.201000689.
[141] R.-H. Shi, Z.-R. Zhang, H.-L. Fan, T. Zhen, J. Shangguan, J. Mi, Cu-based metal–organic framework/activated carbon composites for sulfur compounds removal, Appl. Surf. Sci. 394 (2017) 394–402, https://doi.org/10.1016/j.apsusc.2016.10.071.
[142] M. Kooti, A. Pourreza, A. Rashidi, Preparation of MIL-101-nanoporous carbon as a new type of nanoadsorbent for H2S removal from gas stream, J. Nat. Gas Sci. Eng. 57 (2018) 331–338, https://doi.org/10.1016/j.jngse.2018.07.015.
[143] M. Daraee, R. Saeedirad, A. Rashidi, Adsorption of hydrogen sulfide over a novel metal organic framework –metal oxide nanocomposite: TOUO-x (TiO2/UiO-66), J. Solid State Chem. 278 (2019) 120866, https://doi.org/10.1016/j.jssc.2019.07.027.
[144] V. Rodin, J. Lindorfer, H. Böhm, L. Vieira, Assessing the potential of carbon dioxide valorisation in Europe with focus on biogenic CO2, J. CO2 Util. 41 (2020) 101219, https://doi.org/10.1016/j.jcou.2020.101219.
[145] Q. Sun, H. Li, J. Yan, L. Liu, Z. Yu, X. Yu, Selection of appropriate biogas upgrading technology-a review of biogas cleaning, upgrading and utilisation, Renew. Sustain. Energy Rev. 51 (2015) 521–532, https://doi.org/10.1016/j.rser.2015.06.029.
[146] I. Bragança, F. Sánchez-Soberón, G.F. Pantuzza, A. Alves, N. Ratola, Impurities in biogas: analytical strategies, occurrence, effects and removal technologies, Biomass Bioenergy 143 (2020) 105878, https://doi.org/10.1016/j.biombioe.2020.105878.
[147] P. Tanvidkar, S. Appari, B.V.R. Kuncharam, A review of techniques to improve performance of metal organic framework (MOF) based mixed matrix membranes for CO2/CH4 separation, Rev. Environ. Sci. Biotechnol. 21 (2022) 539–569, https://doi.org/10.1007/s11157-022-09612-5.
[148] M. Karimi, A. Ferreira, A.E. Rodrigues, F. Nouar, C. Serre, J.A.C. Silva, MIL-160 (Al) as a candidate for biogas upgrading and CO2 capture by adsorption processes, Ind. Eng. Chem. Res. 62 (2023) 5216–5229, https://doi.org/10.1021/acs.iecr.2c04150.
[149] B. Ghalei, K. Sakurai, Y. Kinoshita, K. Wakimoto, A.P. Isfahani, Q. Song, K. Doitomi, S. Furukawa, H. Hirao, H. Kusuda, S. Kitagawa, E. Sivaniah, Enhanced selectivity in mixed matrix membranes for CO2 capture through efficient dispersion of amine-functionalized MOF nanoparticles, Nat. Energy 2 (2017) 17086, https://doi.org/10.1038/nenergy.2017.86.
[150] Z. Qiao, N. Wang, J. Jiang, J. Zhou, Design of amine-functionalized metal–organic frameworks for CO2 separation: the more amine, the better? Chem. Commun. 52 (2016) 974–977, https://doi.org/10.1039/C5CC07171B.
[151] X. Guo, H. Huang, Y. Ban, Q. Yang, Y. Xiao, Y. Li, W. Yang, C. Zhong, Mixed matrix membranes incorporated with amine-functionalized titanium-based metal-organic framework for CO2/CH4 separation, J. Membr. Sci. 478 (2015) 130–139, https://doi.org/10.1016/j.memsci.2015.01.007.
[152] Y. Lin, C. Kong, L. Chen, Amine-functionalized metal–organic frameworks: structure, synthesis and applications, RSC Adv. 6 (2016) 32598–32614, https://doi.org/10.1039/C6RA01536K.
[153] I. Erucar, S. Keskin, High CO2 selectivity of an amine-functionalized metal organic framework in adsorption-based and membrane-based gas separations, Ind. Eng. Chem. Res. 52 (2013) 3462–3472, https://doi.org/10.1021/ie303343m.
[154] M. Jia, Y. Feng, J. Qiu, X.-F. Zhang, J. Yao, Amine-functionalized MOFs@GO as filler in mixed matrix membrane for selective CO2 separation, Separ. Purif. Technol. 213 (2019) 63–69, https://doi.org/10.1016/j.seppur.2018.12.029.
[155] M.L. Foo, R. Matsuda, Y. Hijikata, R. Krishna, H. Sato, S. Horike, A. Hori, J. Duan, Y. Sato, Y. Kubota, M. Takata, S. Kitagawa, An adsorbate discriminatory gate effect in a flexible porous coordination polymer for selective adsorption of CO2 over C2H2, J. Am. Chem. Soc. 138 (2016) 3022–3030, https://doi.org/10.1021/jacs.5b10491.
[156] M.K. Taylor, T. Runčevski, J. Oktawiec, J.E. Bachman, R.L. Siegelman, H. Jiang, J. A. Mason, J.D. Tarver, J.R. Long, Near-perfect CO2/CH4 selectivity achieved through reversible guest templating in the flexible metal–organic framework Co (bdp), J. Am. Chem. Soc. 140 (2018) 10324–10331, https://doi.org/10.1021/jacs.8b06062.
[157] H.R. Mahdipoor, R. Halladj, E. Ganji Babakhani, S. Amjad-Iranagh, J. Sadeghzadeh Ahari, Adsorption of CO2, N2 and CH4 on a Fe-based metal organic framework, MIL-101(Fe)-NH2, Colloids Surf. A Physicochem. Eng. Asp. 619 (2021) 126554, https://doi.org/10.1016/j.colsurfa.2021.126554.
[158] C. Chen, X. Li, W. Zou, H. Wan, L. Dong, G. Guan, Structural modulation of UiO-66-NH2 metal-organic framework via interligands cross-linking: cooperative effects of pore diameter and amide group on selective CO2 separation, Appl. Surf. Sci. 553 (2021) 149547, https://doi.org/10.1016/j.apsusc.2021.149547.
[159] A. Phan, C.J. Doonan, F.J. Uribe-Romo, C.B. Knobler, M. O'Keeffe, O.M. Yaghi, Synthesis, structure, and carbon dioxide capture properties of zeolitic imidazolate frameworks, Acc. Chem. Res. 43 (2010) 58–67, https://doi.org/10.1021/ar900116g.
[160] H.P. Paudel, W. Shi, D. Hopkinson, J.A. Steckel, Y. Duan, Computational modelling of adsorption and diffusion properties of CO2 and CH4 in ZIF-8 for gas separation applications: a density functional theory approach, React. Chem. Eng. 6 (2021) 990–1001, https://doi.org/10.1039/D0RE00416B.
[161] K.S. Park, Z. Ni, A.P. Côté, J.Y. Choi, R. Huang, F.J. Uribe-Romo, H.K. Chae, M. O'Keeffe, O.M. Yaghi, Exceptional chemical and thermal stability of zeolitic imidazolate frameworks, Proc. Natl. Acad. Sci. USA 103 (2006) 10186–10191, https://doi.org/10.1073/pnas.0602439103.
[162] H.N. Abdelhamid, Removal of carbon dioxide using zeolitic imidazolate frameworks: adsorption and conversion via catalysis, Appl. Organomet. Chem. 36 (2022) e6753, https://doi.org/10.1002/aoc.6753.
[163] H.N. Abdelhamid, Salts induced formation of hierarchical porous ZIF-8 and their applications for CO2 sorption and hydrogen generation via NaBH4 hydrolysis, Macromol. Chem. Phys. 221 (2020) 2000031, https://doi.org/10.1002/macp.202000031.

[164] H. Nasser Abdelhamid, A.P. Mathew, Cellulose-zeolitic imidazolate frameworks (CelloZIFs) for multifunctional environmental remediation: adsorption and catalytic degradation, Chem. Eng. J. 426 (2021) 131733, https://doi.org/10.1016/j.cej.2021.131733.
[165] A. Huang, Q. Liu, N. Wang, Y. Zhu, J. Caro, Bicontinuous zeolitic imidazolate framework ZIF-8@GO membrane with enhanced hydrogen selectivity, J. Am. Chem. Soc. 136 (2014) 14686–14689, https://doi.org/10.1021/ja5083602.
[166] J.H. Aldrich, S.M. Rousselo, M.L. Yang, S.M. Araiza, F. Tian, Adsorptive separation of methane from carbon dioxide by zeolite@ZIF composite, Energy Fuel. 33 (2019) 348–355, https://doi.org/10.1021/acs.energyfuels.8b03484.
[167] B.R. Pimentel, A. Parulkar, E. Zhou, N.A. Brunelli, R.P. Lively, Zeolitic imidazolate frameworks: next-generation materials for energy-efficient gas separations, ChemSusChem 7 (2014) 3202–3240, https://doi.org/10.1002/cssc.201402647.
[168] F. Bai, Y. Xia, B. Chen, H. Su, Y. Zhu, Preparation and carbon dioxide uptake capacity of N-doped porous carbon materials derived from direct carbonization of zeolitic imidazolate framework, Carbon 79 (2014) 213–226, https://doi.org/10.1016/j.carbon.2014.07.062.
[169] S. Ullah, M.A. Bustam, M.A. Assiri, A.G. Al-Sehemi, F.A. Abdul Kareem, A. Mukhtar, M. Ayoub, G. Gonfa, Synthesis and characterization of iso-reticular metal-organic Framework-3 (IRMOF-3) for CO2/CH4 adsorption: impact of post-synthetic aminomethyl propanol (AMP) functionalization, J. Nat. Gas Sci. Eng. 72 (2019) 103014, https://doi.org/10.1016/j.jngse.2019.103014.
[170] A.R. Millward, O.M. Yaghi, Metal−Organic frameworks with exceptionally high capacity for storage of carbon dioxide at room temperature, J. Am. Chem. Soc. 127 (2005) 17998–17999, https://doi.org/10.1021/ja0570032.
[171] C. Chen, X. Li, W. Zou, H. Wan, L. Dong, G. Guan, Structural modulation of UiO-66-NH2 metal-organic framework via interligands cross-linking: cooperative effects of pore diameter and amide group on selective CO2 separation, Appl. Surf. Sci. 553 (2021) 149547, https://doi.org/10.1016/j.apsusc.2021.149547.
[172] I.K. Shamsudin, I. Idris, A. Abdullah, J. Kim, M.R. Othman, Development of microporous Zr-MOF UiO-66 by sol-gel synthesis for CO2 capture from synthetic gas containing CO2 and H2, AIP Conf. Proc. 2124 (2019) 020057, https://doi.org/10.1063/1.5117117.
[173] A. Noushadi, F. Fotovat, T. Hamzehlouyan, M. Vahidi, Application of an amino-functionalized MIL-53(Al) MOF as an efficient, selective, and durable adsorbent for SO2 removal, J. Environ. Chem. Eng. 10 (2022) 108768, https://doi.org/10.1016/j.jece.2022.108768.
[174] F. Rezaei, S. Lawson, H. Hosseini, H. Thakkar, A. Hajari, S. Monjezi, A. A. Rownaghi, MOF-74 and UTSA-16 film growth on monolithic structures and their CO2 adsorption performance, Chem. Eng. J. 313 (2017) 1346–1353, https://doi.org/10.1016/j.cej.2016.11.058.
[175] Y. Mao, D. Chen, P. Hu, Y. Guo, Y. Ying, W. Ying, X. Peng, Hierarchical mesoporous metal–organic frameworks for enhanced CO2 capture, Chem. Eur J. 21 (2015) 15127–15132, https://doi.org/10.1002/chem.201502515.
[176] S. Chand Pal, R. Krishna, M.C. Das, Highly scalable acid-base resistant Cu-Prussian blue metal-organic framework for C2H2/C2H4, biogas, and flue gas separations, Chem. Eng. J. 460 (2023) 141795, https://doi.org/10.1016/j.cej.2023.141795.
[177] S. Chaemchuen, K. Zhou, N.A. Kabir, Y. Chen, X. Ke, G. Van Tendeloo, F. Verpoort, Tuning metal sites of DABCO MOF for gas purification at ambient conditions, Microporous Mesoporous Mater. 201 (2015) 277–285, https://doi.org/10.1016/j.micromeso.2014.09.038.
[178] H. Furukawa, N. Ko, Y.B. Go, N. Aratani, S.B. Choi, E. Choi, A.Ö. Yazaydin, R. Q. Snurr, M. O'Keeffe, J. Kim, O.M. Yaghi, Ultrahigh porosity in metal-organic frameworks, Science 329 (2010) 424–428, https://doi.org/10.1126/science.1192160.
[179] Y. Lin, C. Kong, L. Chen, Direct synthesis of amine-functionalized MIL-101(Cr) nanoparticles and application for CO2 capture, RSC Adv. 2 (2012) 6417–6419, https://doi.org/10.1039/C2RA20641B.
[180] A. Taheri, E. Ganji Babakhani, J. Towfighi Darian, S. Pakseresht, Hybrid MIL-101 (Cr)@MIL-53(Al) composite for carbon dioxide capture from biogas, RSC Adv. 9 (2019) 15141–15150, https://doi.org/10.1039/C8RA10619C.
[181] S. Couck, J.F.M. Denayer, G.V. Baron, T. Rémy, J. Gascon, F. Kapteijn, An amine-functionalized MIL-53 Metal−Organic framework with large separation power for CO2 and CH4, J. Am. Chem. Soc. 131 (2009) 6326–6327, https://doi.org/10.1021/ja900555r.
[182] H.E. Emam, R.M. Abdelhameed, H.B. Ahmed, Adsorptive performance of MOFs and MOF containing composites for clean energy and safe environment, J. Environ. Chem. Eng. 8 (2020) 104386, https://doi.org/10.1016/j.jece.2020.104386.
[183] J. Liu, C. Chen, K. Zhang, L. Zhang, Applications of metal–organic framework composites in CO2 capture and conversion, Chin. Chem. Lett. 32 (2021) 649–659, https://doi.org/10.1016/j.cclet.2020.07.040.
[184] Y. Zhao, H. Ding, Q. Zhong, Synthesis and characterization of MOF-aminated graphite oxide composites for CO2 capture, Appl. Surf. Sci. 284 (2013) 138–144, https://doi.org/10.1016/j.apsusc.2013.07.068.
[185] Y. Zhao, M. Seredych, Q. Zhong, T.J. Bandosz, Superior performance of copper based MOF and aminated graphite oxide composites as CO2 adsorbents at room temperature, ACS Appl. Mater. Interfaces 5 (2013) 4951–4959, https://doi.org/10.1021/am4006989.
[186] A. Policicchio, Y. Zhao, Q. Zhong, R.G. Agostino, T.J. Bandosz, Cu-BTC/Aminated graphite oxide composites as high-efficiency CO2 capture media, ACS Appl. Mater. Interfaces 6 (2014) 101–108, https://doi.org/10.1021/am404952z.
[187] D. Qian, C. Lei, G.-P. Hao, W.-C. Li, A.-H. Lu, Synthesis of hierarchical porous carbon monoliths with incorporated metal–organic frameworks for enhancing volumetric based CO2 capture capability, ACS Appl. Mater. Interfaces 4 (2012) 6125–6132, https://doi.org/10.1021/am301772k.
[188] Y. Zhao, M. Seredych, Q. Zhong, T.J. Bandosz, Aminated graphite oxides and their composites with copper-based metal–organic framework: in search for efficient media for CO2 sequestration, RSC Adv. 3 (2013) 9932–9941, https://doi.org/10.1039/C3RA40817E.
[189] C. Petit, J. Burress, T.J. Bandosz, The synthesis and characterization of copper-based metal–organic framework/graphite oxide composites, Carbon 49 (2011) 563–572, https://doi.org/10.1016/j.carbon.2010.09.059.
[190] Y. Cao, Y. Zhao, Z. Lv, F. Song, Q. Zhong, Preparation and enhanced CO2 adsorption capacity of UiO-66/graphene oxide composites, J. Ind. Eng. Chem. 27 (2015) 102–107, https://doi.org/10.1016/j.jiec.2014.12.021.
[191] B. Szczęśniak, J. Choma, Graphene-containing microporous composites for selective CO2 adsorption, Microporous Mesoporous Mater. 292 (2020) 109761, https://doi.org/10.1016/j.micromeso.2019.109761.
[192] A. Borrás, A. Rosado, J. Fraile, A.M. López-Periago, J. Giner Planas, A. Yazdi, C. Domingo, Meso/microporous MOF@graphene oxide composite aerogels prepared by generic supercritical CO2 technology, Microporous Mesoporous Mater. 335 (2022) 111825, https://doi.org/10.1016/j.micromeso.2022.111825.
[193] Q. Hou, S. Zhou, Y. Wei, J. Caro, H. Wang, Balancing the grain boundary structure and the framework flexibility through bimetallic metal–organic framework (MOF) membranes for gas separation, J. Am. Chem. Soc. 142 (2020) 9582–9586, https://doi.org/10.1021/jacs.0c02181.
[194] K.B. Idrees, Z. Chen, X. Zhang, M.R. Mian, R.J. Drout, T. Islamoglu, O.K. Farha, Tailoring pore aperture and structural defects in zirconium-based metal–organic frameworks for krypton/xenon separation, Chem. Mater. 32 (2020) 3776–3782, https://doi.org/10.1021/acs.chemmater.9b05048.
[195] M.R. Abdul Hamid, Y. Qian, R. Wei, Z. Li, Y. Pan, Z. Lai, H.-K. Jeong, Polycrystalline metal-organic framework (MOF) membranes for molecular separations: engineering prospects and challenges, J. Membr. Sci. 640 (2021) 119802, https://doi.org/10.1016/j.memsci.2021.119802.
[196] Y. Pan, B. Wang, Z. Lai, Synthesis of ceramic hollow fiber supported zeolitic imidazolate framework-8 (ZIF-8) membranes with high hydrogen permeability, 421–422, J. Membr. Sci. (2012) 292–298, https://doi.org/10.1016/j.memsci.2012.07.028.
[197] Y. Wang, H. Jin, Q. Ma, K. Mo, H. Mao, A. Feldhoff, X. Cao, Y. Li, F. Pan, Z. Jiang, A MOF glass membrane for gas separation, Angew. Chem. Int. Ed. 59 (2020) 4365–4369, https://doi.org/10.1002/anie.201915807.
[198] D.-S. Chiou, H.J. Yu, T.-H. Hung, Q. Lyu, C.-K. Chang, J.S. Lee, L.-C. Lin, D.-Y. Kang, Highly CO2 selective metal–organic framework membranes with favorable coulombic effect, Adv. Funct. Mater. 31 (2021) 2006924, https://doi.org/10.1002/adfm.202006924.
[199] T.-M.T. Nguyen, J.-W. Chen, M.-T. Pham, H.M. Bui, C.-C. Hu, S.-J. You, Y.-F. Wang, A high-performance ZIF-8 membrane for gas separation applications: synthesis and characterization, Environ. Technol. Innovat. 31 (2023) 103169, https://doi.org/10.1016/j.eti.2023.103169.
[200] A. Huang, Q. Liu, N. Wang, J. Caro, Highly hydrogen permselective ZIF-8 membranes supported on polydopamine functionalized macroporous stainless-steel-nets, J. Mater. Chem. A 2 (2014) 8246–8251, https://doi.org/10.1039/C4TA00299G.
[201] S.R. Venna, M.A. Carreon, Highly permeable zeolite imidazolate framework-8 membranes for CO2/CH4 separation, J. Am. Chem. Soc. 132 (2010) 76–78, https://doi.org/10.1021/ja909263x.
[202] P. Nian, Y. Cao, Y. Li, X. Zhang, Y. Wang, H. Liu, X. Zhang, Preparation of a pure ZIF-67 membrane by self-conversion of cobalt carbonate hydroxide nanowires for H2 separation, CrystEngComm 20 (2018) 2440–2448, https://doi.org/10.1039/C8CE00238J.
[203] H. Chen, C. Li, L. Liu, B. Meng, N. Yang, J. Sunarso, L. Liu, S. Liu, X. Wang, ZIF-67 membranes supported on porous ZnO hollow fibers for hydrogen separation from gas mixtures, J. Membr. Sci. 653 (2022) 120550, https://doi.org/10.1016/j.memsci.2022.120550.
[204] Y. Pan, B. Wang, Z. Lai, Synthesis of ceramic hollow fiber supported zeolitic imidazolate framework-8 (ZIF-8) membranes with high hydrogen permeability, 421–422, J. Membr. Sci. (2012) 292–298, https://doi.org/10.1016/j.memsci.2012.07.028.
[205] Y.-S. Li, F.-Y. Liang, H. Bux, A. Feldhoff, W.-S. Yang, J. Caro, Molecular sieve membrane: supported metal–organic framework with high hydrogen selectivity, Angew. Chem. Int. Ed. 49 (2010) 548–551, https://doi.org/10.1002/anie.200905645.
[206] M.R. Abdul Hamid, H.-K. Jeong, Flow synthesis of polycrystalline ZIF-8 membranes on polyvinylidene fluoride hollow fibers for recovery of hydrogen and propylene, J. Ind. Eng. Chem. 88 (2020) 319–327, https://doi.org/10.1016/j.jiec.2020.04.031.
[207] Z. Rui, J.B. James, A. Kasik, Y.S. Lin, Metal-organic framework membrane process for high purity CO2 production, AIChE J. 62 (2016) 3836–3841, https://doi.org/10.1002/aic.15367.
[208] S.S. Hosseini, M. Azadi Tabar, I.F.J. Vankelecom, J.F.M. Denayer, Progress in high performance membrane materials and processes for biogas production, upgrading and conversion, Separ. Purif. Technol. 310 (2023) 123139, https://doi.org/10.1016/j.seppur.2023.123139.
[209] K. Scott, R. Hughes, Introduction to industrial membrane processes, in: K. Scott, R. Hughes (Eds.), Industrial Membrane Separation Technology, Springer Netherlands, Dordrecht, 1996, pp. 1–7, https://doi.org/10.1007/978-94-011-0627-6_1.

[210] J.K. Adewole, A.L. Ahmad, S. Ismail, C.P. Leo, Current challenges in membrane separation of CO2 from natural gas: a review, Int. J. Greenh. Gas Control 17 (2013) 46–65, https://doi.org/10.1016/j.ijggc.2013.04.012.
[211] N. Fajrina, N. Yusof, A.F. Ismail, F. Aziz, M.R. Bilad, M. Alkahtani, A crucial review on the challenges and recent gas membrane development for biogas upgrading, J. Environ. Chem. Eng. 11 (2023) 110235, https://doi.org/10.1016/j.jece.2023.110235.
[212] G. Liu, A. Cadiau, Y. Liu, K. Adil, V. Chernikova, I.-D. Carja, Y. Belmabkhout, M. Karunakaran, O. Shekhah, C. Zhang, A.K. Itta, S. Yi, M. Eddaoudi, W.J. Koros, Enabling fluorinated MOF-based membranes for simultaneous removal of H2S and CO2 from natural gas, Angew. Chem. Int. Ed. 57 (2018) 14811–14816, https://doi.org/10.1002/anie.201808991.
[213] S. Wang, D. Wu, H. Huang, Q. Yang, M. Tong, D. Liu, C. Zhong, Computational exploration of H2S/CH4 mixture separation using acid-functionalized UiO-66(Zr) membrane and composites, Chin. J. Chem. Eng. 23 (2015) 1291–1299, https://doi.org/10.1016/j.cjche.2015.04.017.
[214] S.J. Datta, A. Mayoral, N. Murthy Srivatsa Bettahalli, P.M. Bhatt, M. Karunakaran, I.D. Carja, D. Fan, P. Graziane M. Mileo, R. Semino, G. Maurin, O. Terasaki, M. Eddaoudi, Rational design of mixed-matrix metal-organic framework membranes for molecular separations, Science 376 (2022) 1080–1087, https://doi.org/10.1126/science.abe0192.
[215] L. Zhao, Z. Liu, Z. Wang, S.J.D. Smith, X. Lu, C. Wu, D. Ng, J. Zhang, Q.J. Niu, Z. Xie, MOF incorporated adsorptive nanofibrous membranes for enhanced ammonia removal by membrane distillation, Desalination 568 (2023) 117018, https://doi.org/10.1016/j.desal.2023.117018.
[216] J.B. DeCoste Jr., S. Denny Michael, G.W. Peterson, J.J. Mahle, S.M. Cohen, Enhanced aging properties of HKUST-1 in hydrophobic mixed-matrix membranes for ammonia adsorption, Chem. Sci. 7 (2016) 2711–2716, https://doi.org/10.1039/C5SC04368A.
[217] J. Zhang, Z. Huang, L. Gao, S. Gray, Z. Xie, Study of MOF incorporated dual layer membrane with enhanced removal of ammonia and per-/poly-fluoroalkyl substances (PFAS) in landfill leachate treatment, Sci. Total Environ. 806 (2022) 151207, https://doi.org/10.1016/j.scitotenv.2021.151207.
[218] Y. Song, J. Chau, K.K. Sirkar, G.W. Peterson, U. Beuscher, Membrane-supported metal organic framework based nanopacked bed for protection against toxic vapors and gases, Separ. Purif. Technol. 251 (2020) 117406, https://doi.org/10.1016/j.seppur.2020.117406.
[219] X. Guo, H. Huang, Y. Ban, Q. Yang, Y. Xiao, Y. Li, W. Yang, C. Zhong, Mixed matrix membranes incorporated with amine-functionalized titanium-based metal-organic framework for CO2/CH4 separation, J. Membr. Sci. 478 (2015) 130–139, https://doi.org/10.1016/j.memsci.2015.01.007.
[220] T.-H. Bae, J.S. Lee, W. Qiu, W.J. Koros, C.W. Jones, S. Nair, A high-performance gas-separation membrane containing submicrometer-sized metal–organic framework crystals, Angew. Chem. Int. Ed. 49 (2010) 9863–9866, https://doi.org/10.1002/anie.201006141.
[221] B. Zornoza, A. Martinez-Joaristi, P. Serra-Crespo, C. Tellez, J. Coronas, J. Gascon, F. Kapteijn, Functionalized flexible MOFs as fillers in mixed matrix membranes for highly selective separation of CO2 from CH4 at elevated pressures, Chem. Commun. 47 (2011) 9522–9524, https://doi.org/10.1039/C1CC13431K.
[222] M. Waqas Anjum, B. Bueken, D. De Vos, I.F.J. Vankelecom, MIL-125(Ti) based mixed matrix membranes for CO2 separation from CH4 and N2, J. Membr. Sci. 502 (2016) 21–28, https://doi.org/10.1016/j.memsci.2015.12.022.
[223] H. Sanaeepur, A.E. Amooghin, A. Moghadassi, A. Kargari, Preparation and characterization of acrylonitrile–butadiene–styrene/poly(vinyl acetate) membrane for CO2 removal, Separ. Purif. Technol. 80 (2011) 499–508, https://doi.org/10.1016/j.seppur.2011.06.003.
[224] D.J. Harrigan, J. Yang, B.J. Sundell, J.A. Lawrence, J.T. O'Brien, M.L. Ostraat, Sour gas transport in poly(ether-b-amide) membranes for natural gas separations, J. Membr. Sci. 595 (2020) 117497, https://doi.org/10.1016/j.memsci.2019.117497.
[225] R. Nasir, H. Mukhtar, Z. Man, D.F. Mohshim, Material advancements in fabrication of mixed-matrix membranes, Chem. Eng. Technol. 36 (2013) 717–727, https://doi.org/10.1002/ceat.201200734.
[226] Y. Cheng, Y. Ying, S. Japip, S.-D. Jiang, T.-S. Chung, S. Zhang, D. Zhao, Advanced porous materials in mixed matrix membranes, Adv. Mater. 30 (2018) 1802401, https://doi.org/10.1002/adma.201802401.
[227] J. Dechnik, J. Gascon, C.J. Doonan, C. Janiak, C.J. Sumby, Mixed-matrix membranes, Angew. Chem. Int. Ed. 56 (2017) 9292–9310, https://doi.org/10.1002/anie.201701109.
[228] S. Wang, D. Wu, H. Huang, Q. Yang, M. Tong, D. Liu, C. Zhong, Computational exploration of H2S/CH4 mixture separation using acid-functionalized UiO-66(Zr) membrane and composites, Chin. J. Chem. Eng. 23 (2015) 1291–1299, https://doi.org/10.1016/j.cjche.2015.04.017.
[229] J. Wang, Y. Zhou, X. Liu, Q. Liu, M. Hao, S. Wang, Z. Chen, H. Yang, X. Wang, Design and application of metal–organic framework membranes for gas and liquid separations, Separ. Purif. Technol. 329 (2024) 125178, https://doi.org/10.1016/j.seppur.2023.125178.
[230] J. Shen, G. Liu, K. Huang, Q. Li, K. Guan, Y. Li, W. Jin, UiO-66-polyether block amide mixed matrix membranes for CO2 separation, J. Membr. Sci. 513 (2016) 155–165, https://doi.org/10.1016/j.memsci.2016.04.045.
[231] L.M. Robeson, Correlation of separation factor versus permeability for polymeric membranes, J. Membr. Sci. 62 (1991) 165–185, https://doi.org/10.1016/0376-7388(91)80060-J.
[232] L.M. Robeson, The upper bound revisited, J. Membr. Sci. 320 (2008) 390–400, https://doi.org/10.1016/j.memsci.2008.04.030.
[233] M.Z. Ahmad, V. Martin-Gil, V. Perfilov, P. Sysel, V. Fila, Investigation of a new co-polyimide, 6FDA-bisP and its ZIF-8 mixed matrix membranes for CO2/CH4 separation, Separ. Purif. Technol. 207 (2018) 523–534, https://doi.org/10.1016/j.seppur.2018.06.067.
[234] X. Bi, Y. Zhang, F. Zhang, S. Zhang, Z. Wang, J. Jin, MOF nanosheet-based mixed matrix membranes with metal–organic coordination interfacial interaction for gas separation, ACS Appl. Mater. Interfaces 12 (2020) 49101–49110, https://doi.org/10.1021/acsami.0c14639.
[235] H. Gong, T.H. Nguyen, R. Wang, T.-H. Bae, Separations of binary mixtures of CO2/CH4 and CO2/N2 with mixed-matrix membranes containing Zn(pyrz)2 (SiF6) metal-organic framework, J. Membr. Sci. 495 (2015) 169–175, https://doi.org/10.1016/j.memsci.2015.08.018.
[236] H.B. Tanh Jeazet, S. Sorribas, J.M. Román-Marín, B. Zornoza, C. Téllez, J. Coronas, C. Janiak, Increased selectivity in CO2/CH4 separation with mixed-matrix membranes of polysulfone and mixed-MOFs MIL-101(Cr) and ZIF-8, Eur. J. Inorg. Chem. 2016 (2016) 4363–4367, https://doi.org/10.1002/ejic.201600190.
[237] N. Tien-Binh, H. Vinh-Thang, X.Y. Chen, D. Rodrigue, S. Kaliaguine, Crosslinked MOF-polymer to enhance gas separation of mixed matrix membranes, J. Membr. Sci. 520 (2016) 941–950, https://doi.org/10.1016/j.memsci.2016.08.045.
[238] X. Wu, C. Liu, J. Caro, A. Huang, Facile synthesis of molecular sieve membranes following "like grows like" principle, J. Membr. Sci. 559 (2018) 1–7, https://doi.org/10.1016/j.memsci.2018.04.053.
[239] B. Ghalei, K. Sakurai, Y. Kinoshita, K. Wakimoto, A.P. Isfahani, Q. Song, K. Doitomi, S. Furukawa, H. Hirao, H. Kusuda, S. Kitagawa, E. Sivaniah, Enhanced selectivity in mixed matrix membranes for CO2 capture through efficient dispersion of amine-functionalized MOF nanoparticles, Nat. Energy 2 (2017) 17086, https://doi.org/10.1038/nenergy.2017.86.
[240] T. Li, Y. Pan, K.-V. Peinemann, Z. Lai, Carbon dioxide selective mixed matrix composite membrane containing ZIF-7 nano-fillers, 425–426, J. Membr. Sci. (2013) 235–242, https://doi.org/10.1016/j.memsci.2012.09.006.
[241] J. Sánchez-Laínez, I. Gracia-Guillén, B. Zornoza, C. Téllez, J. Coronas, Thin supported MOF based mixed matrix membranes of Pebax® 1657 for biogas upgrade, New J. Chem. 43 (2019) 312–319, https://doi.org/10.1039/C8NJ04769C.
[242] W. Zheng, R. Ding, K. Yang, Y. Dai, X. Yan, G. He, ZIF-8 nanoparticles with tunable size for enhanced CO2 capture of Pebax based MMMs, Separ. Purif. Technol. 214 (2019) 111–119, https://doi.org/10.1016/j.seppur.2018.04.010.
[243] D.-S. Chiou, H.J. Yu, T.-H. Hung, Q. Lyu, C.-K. Chang, J.S. Lee, L.-C. Lin, D.-Y. Kang, Highly CO2 selective metal–organic framework membranes with favorable coulombic effect, Adv. Funct. Mater. 31 (2021) 2006924, https://doi.org/10.1002/adfm.202006924.
[244] MaJ.C. Ordoñez, K.J. Balkus, J.P. Ferraris, I.H. Musselman, Molecular sieving realized with ZIF-8/Matrimid® mixed-matrix membranes, J. Membr. Sci. 361 (2010) 28–37, https://doi.org/10.1016/j.memsci.2010.06.017.
[245] S. Ishaq, R. Tamime, M.R. Bilad, A.L. Khan, Mixed matrix membranes comprising of polysulfone and microporous Bio-MOF-1: preparation and gas separation properties, Separ. Purif. Technol. 210 (2019) 442–451, https://doi.org/10.1016/j.seppur.2018.08.031.
[246] S. Shahid, K. Nijmeijer, High pressure gas separation performance of mixed-matrix polymer membranes containing mesoporous Fe(BTC), J. Membr. Sci. 459 (2014) 33–44, https://doi.org/10.1016/j.memsci.2014.02.009.